Supplementary Information for the Manuscript

"From START to FINISH: Computational Analysis of Cell Cycle Control in Budding Yeast"

Pavel Kraikivski, Katherine C. Chen, Teeraphan Laomettachit, T.M. Murali and John J. Tyson

Supplementary Text

1. Brief description of the molecular mechanisms underlying our mathematical model

The "wiring diagram" of our model is presented in Figure 1 of the main text.

START and FINISH are the crucial checkpoints of the budding yeast cell cycle. At START a yeast cell checks that it is large enough to warrant a new round of DNA replication and division, that its DNA is not damaged by (say) ionizing radiation, and that it is not being signaled by cells of opposite mating type to participate in sexual reproduction. At FINISH a yeast cell checks that its chromosomes are fully replicated, undamaged and properly aligned on the mitotic spindle. If these checkpoints malfunction (i.e., if they permit further progression through the cell cycle under non-permissive conditions), then the cell is likely to produce genetically damaged or inviable progeny.

From START to FINISH, progression through the budding yeast cell cycle is controlled by a cyclin dependent kinase, Cdk1 (encoded by the *CDC28* gene in budding yeast), which interacts with different cyclin partners at different stages of the cell cycle (1, 2). The G1 cyclin Cln3 forms a heterodimer with Cdk1, denoted Cln3:Cdk1, which initiates the START transition in a cell size-dependent manner (3). Early in G1 phase Cln3 molecules are sequestered on the membrane of the endoplasmic reticulum (ER). When the cell reaches a critical size, Cln3:Cdk1 is released from the ER and transported into the cell nucleus. Passage through the START transition is associated with activation of two master transcription factors, SBF and MBF, that up-regulate the expression of many genes involved in DNA replication and division, including additional cyclins: Cln1, Cln2, Clb5 and Clb6. SBF and MBF are initially activated by Cln3:Cdk1 and Bck2 (4-6). Additionally, SBF and MBF activities are promoted by Cln1,2:Cdk1 and Clb5,6:Cdk1, creating positive feedback loops that make the START transition irreversible (7-10). (Cln1,2:Cdk1 is our shorthand for Cln1:Cdk1, Cln2:Cdk1.) After the START transition, the budding yeast cell produces a new bud (driven primarily by Cln2:Cdk1) and initiates DNA synthesis (driven primarily by Clb5:Cdk1). The newly replicated DNA molecules, called sister chromatids, are held together by cohesin rings.

During S/G2/M phase of the division cycle, a budding yeast cell activates a G2/M-specific transcription factor, comprised of Mcm1, Fkh2 and Ndd1, which we abbreviate "MCM1". MCM1 up-regulates production of a suite of regulatory proteins, including the mitotic cyclins (Clb1 and Clb2), the polo-like kinase (Cdc5), securin (Pds1), and a targeting protein (Cdc20). The mitotic cyclin-dependent kinases are essential for entry into mitosis; most notably, for inducing formation of the intra-nuclear mitotic spindle. As the replicated chromosomes are being aligned on the metaphase plate of the spindle, premature separation of the pairs of sister chromatids is prevented by Pds1, which binds to and inhibits Esp1 (separase), the protease responsible for cleavage of the cohesin rings. Cdc20 is a partner of the Anaphase Promoting Complex (APC), an E3 ubiquitin ligase that is responsible for the ordered degradation of proteins during anaphase and telophase. Prior to anaphase, the Mitotic Checkpoint Complex (MCC) prevents Cdc20:APC from ubiquitinating Clb1,2 or Pds1. When all chromosomes are properly aligned on the metaphase plate, the cell is ready to finish the cell cycle.

Like START, the FINISH transition is associated with a number of processes that occur in rapid, overlapping steps. As the MCC inactivates, Cdc20:APC labels Pds1 for proteolysis. Pds1 degradation releases Esp1, which cleaves the cohesin rings that are holding together sister chromatid pairs. Consequently, the mitotic spindle pulls the sister chromatids to opposite sides of the cell (half the chromosomes are pulled back into the mother cell, and half are pushed into the bud). Cdc20:APC also initiates degradation of the mitotic cyclins. In addition, resetting the budding yeast cell to G1 phase requires activation of a powerful phosphatase, Cdc14, which reverses the phosphorylations that have built up during S/G2/M by the action of cyclin:Cdk1 complexes. Cdc14 is kept inactive by binding to an inhibitor, Net1. As cells exit from mitosis, Net1 is phosphorylated and inactivated, and Cdc14 is released. Net1 phosphorylation and Cdc14 release occur in two stages: early, transient release is driven by Clb2:Cdk1 and by Cdc5 (polo-kinase), and later, full release is driven by kinases of the Mitotic Exit Network (MEN). MEN activation requires proper positioning of the metaphase nucleus in the bud neck, with the old spindle pole oriented toward the mother cell and the new spindle pole oriented toward the daughter cell. Improper positioning of the spindle axis will invoke the "Spindle POsition Checkpoint" (SPOC), which prevents activation of the MEN, thereby delaying cell division and giving the cell a chance to reorient the anaphase spindle. (We will not attempt to model the SPOC in this paper, but we will put a "socket" in the model for future insertion of a SPOC module.)

Once the cell is reset to G1, the kinases are all inactivated, Net1 is dephosphorylated, and Cdc14 is re-sequestered in the inactive Cdc14:Net1 complex.

2. Mathematical Model

The wiring diagram of our model contains three basic types of chemical reactions: protein synthesis and degradation ($\rightarrow C \rightarrow$), phosphorylation and de-phosphorylation ($C \leftrightarrow C_P$), and the formation of protein complexes ($C + A \leftrightarrow C{:}A$). These three types of reactions typically proceed

on different time scales. Protein levels change, due to synthesis and degradation, on a time scale of 10's of minutes. The phosphorylation state of a protein can change in minutes or less. Protein complexes can form and dissolve within seconds. To support this assumption of three disparate time scales, we refer to an earlier model of the budding yeast cell cycle (11), which made no *a priori* assumptions about rate constant values. Nonetheless, in fitting this model to yeast cell phenotypes, Chen et al. were led to rate constants for protein synthesis and degradation with values ~0.1 min^{-1}, rate constants for protein activation and inactivation with values ~1 min^{-1}, and rate constants for association of protein complexes with values ~50 min^{-1}. In a similar study of cell cycle regulation in frog egg extracts, Marlovits et al. (12) fitted their model to experimental data with rate constants for protein synthesis and degradation of ~0.01 min^{-1} and rate constants for protein phosphorylation and dephosphorylation of ~0.5 min^{-1}. In this case, however, they estimated that the rate constant for association of Cdk1 with cyclin B was rather slow, ~0.5 min^{-1}. In cases where reaction rates do not scale as we assume, one can always revert to a more accurate representation of the reaction kinetics, e.g., mass-action rate laws.

For each of these three standard types of reaction we use a specific mathematical representation appropriate for its biochemistry and kinetics (13). Protein synthesis and degradation are modeled by the differential equation

$$\frac{dC_{\mathrm{T}}}{dt} = k_{\mathrm{s0}} + \sum_i k_{\mathrm{s}i} X_i - \left(k_{\mathrm{d0}} + \sum_j k_{\mathrm{d}j} X_j\right) C_{\mathrm{T}},$$

where C_{T} = total concentration of species C, X_i = activity of transcription factors for species C, and X_j = activity of proteases for species C. The rate constants for protein synthesis and degradation, $k_{\mathrm{s}i}$ and $k_{\mathrm{d}j}$, respectively, are numbers of order-of-magnitude 0.1 min^{-1}.

Protein phosphorylation and dephosphorylation are modeled by the differential equation

$$\frac{dC_{\mathrm{P}}}{dt} = \gamma\left(\frac{C_{\mathrm{T}}}{1+e^{-\sigma W}} - C_{\mathrm{P}}\right),$$

where $W = \omega_0 + \sum_i \omega^{\mathrm{K}}{}_i K_i - \sum_j \omega^{\mathrm{H}}{}_j H_j$, the ω^{K}'s and ω^{H}'s are positive "interaction coefficients", K_i and H_j are the activities of the kinases and phosphatases the modify C, and γ is a rate constant. The "soft-Heaviside" function, $1/(1+e^{-\sigma W})$, is a sigmoidal function that varies from 0 for $W << -1/\sigma$ to 0.5 for $W = 0$ to 1 for $W >> 1/\sigma$. Clearly, σ controls the sharpness of the transition from 0 and 1 as W passes through 0, provided the ω's are scaled to values of order 1. The "basal" interaction coefficient ω_0 (which may be positive, negative or zero) determines whether C is phosphorylated or not when it is receiving no input from the kinases and phosphatases. The rate constant $\gamma > 0$ controls how fast C_{P} approaches its pseudo-steady state value $C_{\mathrm{T}}/(1+\mathrm{e}^{-\sigma W})$. Soft-Heaviside functions have been used by other authors to model sigmoidal signal-response curves in molecular cell biology (14, 15).

If protein C binds tightly to a stoichiometric binding partner A, then C_F, the concentration of the free form of the protein C, is given by:

$$C_F = \max(0, C_T - A_T) .$$

This modeling approach is modular and quantitative, while keeping the number of adjustable parameters per reaction step to a minimum. It exploits the characteristic types of reactions that control the activities of cyclin-dependent kinases; namely, synthesis and degradation of cyclins, phosphorylation and dephosphorylation of target proteins, and strong association of protein binding partners. As the σ and γ parameters tend to $+\infty$, the C_P variables constitute a Boolean switching network, and the C_T variables are governed by "piecewise linear" ODEs. In this limit, our intuitive feel for switching networks serves pretty well (16-18). For σ and γ large (but finite), our network is governed by nonlinear ODEs with continuous rate functions, and we have access to all the power of dynamical systems theory and bifurcation analysis. The modularity of the model makes it relatively easy to add new modules to extend the model to describe additional aspects of the control network.

A data-mining approach called LINKER (19) was used to interrogate the model and suggest new modules for incorporation. LINKER accesses public repositories of experimental data on budding yeast genes and proteins, and preprocesses that data for their relevance to the cell cycle. Starting with a "core" of cell cycle control proteins (from the 2004 Chen model of the budding yeast cell cycle), LINKER identifies a set of potentially relevant proteins linked to the core by physical interactions, phosphorylation relationships, or other types of interactions. Then LINKER's auxiliary tool, GraphSpace, represents sets of potentially cell cycle-related proteins and interactions as graphs. Building a cell cycle interactome using this approach facilitated the development of the present model. In particular, it elucidated a role for Cdc5 (which is not in 2004 Chen model) in bringing Cdc15 to the spindle pole body where it is necessary to activate MEN kinase (19, 20).

Growth and Division

We assume that cell "size" (mass or volume) increases exponentially in time at a specific growth rate, μ, that depends on the growth medium. In glucose medium, $\mu = 0.0077$ min^{-1} (mass doubling time = 90 min), and in galactose medium $\mu = 0.0046$ min^{-1} (mass doubling time = 150 min). Budding yeast cells divide asymmetrically, with a certain fraction f of division mass going to the daughter cell at division. We compute f from the equation $f = 0.3584e^{32\mu}$ which was derived by Chen et al. (21) from experimental data. In glucose medium, $f = 0.4586$, and in galactose medium, $f = 0.4156$.

Events and Checkpoints

Discontinuous cell cycle events are used as landmarks to monitor cell cycle progress and/or synchrony of a population of cells. They are also used to describe the phenotypes of mutant cells

that arrest in a certain stage of the cell cycle, that delay or skip an event, or that bypass a checkpoint. In the model, cell division occurs when the concentration of mitotic cyclin Clb2 drops below a threshold value (θ_{cd}), which corresponds to about 10% of the maximum Clb2 concentration in a wild-type cell. The events of DNA synthesis initiation, bud emergence and complete alignment of replicated chromosomes on the mitotic spindle are governed (in the model) by the dimensionless variables ORI, BUD and SPN, respectively. The event occurs when the corresponding variable reaches 1. The values of BUD and SPN are reset to zero at cell division, and ORI is reset to zero when total concentration of Clb2 and Clb5 drops below θ_{rl} (rl for "relicensing"), which is set at ~5% of the maximum value of Clb5+Clb2 in a wild-type cell.

The spindle assembly checkpoint (SAC) controls the activity of the Mad2 complex. In the model, SAC is a Boolean variable: SAC = 0 in G1 phase; SAC = 1 from the time of initiation of DNA synthesis (ORI = 1) until the time of complete alignment of chromosomes on the spindle (SPN = 1). Mad2 is activated when SAC = 1.

To model the spindle position checkpoint (SPOC), we introduce an indicator variable, $I_{SPOC} = 1$ when the two conditions of the SPOC are satisfied: (a) the mitotic spindle is properly oriented, with one pole on the mother-side of the bud neck and the other pole on the daughter-side, and (b) cohesin rings are cleaved, allowing the mitotic spindle to push the poles into the mother and daughter compartments.

$$I_{SPOC} = \mathrm{SPO} \cdot \mathrm{Heav}(\mathrm{Esp1}+\mathrm{TEV}-\theta_{cleave})] \cdot (1-\mathrm{NOC}) \, .$$

Here, Heav(x) is the Heaviside function (= 0 if $x \leq 0$; = 1 if $x > 0$); SPO = 1 if the spindle is properly oriented, = 0 otherwise; θ_{cleave} is a threshold activity of protease necessary to cleave cohesin rings; TEV is a Boolean variable (0 or 1) indicating whether or not the Tobacco Etch Virus protease is being expressed in a cell; and NOC is a Boolean variable indicating whether or not the cell is exposed to nocodazole, a microtubule depolymerizing drug. SPO is a "place holder" for a more detailed model (yet to come) of the spindle orientation surveillance mechanism; in the present model we assume that all spindles are properly oriented, i.e., SPO = 1. Esp1 ("separase") is the protease that normally cleaves cohesin rings, but in some experiments where Esp1 is missing or inactivated, a substitute protease, TEV, is used to cleave cohesin rings that have been engineered to carry TEV cleavage sites. When NOC = 1, there are no microtubules to segregate the chromosomes into mother and daughter cells, so $I_{SPOC} = 0$. When $I_{SPOC} = 1$, the checkpoint protein, Bub2, is down-regulated; see Eq. 57 in Table S2. Deactivation of Bub2 is necessary to initiate the mitotic exit network (MEN).

Simulation of Wild-type Yeast Cells

Table S1 lists all the variables we use to describe the wiring diagrams in Figure 1, and Table S2 provides the differential and algebraic equations governing these variables, derived from the wiring diagram according to our approach for modeling Types 1, 2 and 3 reactions. Table S3

provides a basal set of parameter values for simulating wild-type cells growing in glucose medium (see Figure 2 in the main text).

As a check on our simulations, we integrated our simulated curves over a full cell cycle, to compute the following ratios for the average number of molecules per cell in an asynchronous culture of budding yeast:

$$(\text{Cln1} + \text{Cln2}) : (\text{Clb1} + \text{Clb2}) : (\text{Clb5} + \text{Clb6}) : (\text{Sic1} + \text{Cdc6}) = 5.1 : 1.3 : 1 : 0.6 \ .$$

(In an asynchronous culture there are twice as many cells at the beginning of the cell cycle as there are at the end, but they are only half the size. So a simple time-average of species concentration over one cycle should give a good estimate of the average number of molecules of that species in an asynchronous population.) Our computed numbers can be compared to measurements of Cross and colleagues (22, 23) of the average number of protein molecules per cell in an asynchronous culture of diploid yeast cells. Their measured values, in multiples of 876 molecules per cell, are:

$$(\text{Cln1} + \text{Cln2}) : (\text{Clb1} + \text{Clb2}) : (\text{Clb5} + \text{Clb6}) : (\text{Sic1} + \text{Cdc6}) =$$
$$(1.1 + 2.3) : (0.6 + 1.3) : (0.9 + 0.1) : (0.2 + 0.8) = 4.4 : 1.9 : 1 : 1 \ .$$

Although the computed ratios could presumably be brought into closer agreement with the measured ratios by adjusting the rate constants for protein synthesis, we have not tried to do so, considering that the measurements are quite uncertain (the coefficients of variation of Cross's measurements are ~50%). The uncertainty in these ratios is underscored by a separate study of protein expression in yeast cells by Ghaemmaghami et al. (24) who reported the following values, in multiples of 521 molecules per cell:

$$(\text{Cln1} + \text{Cln2}) : (\text{Clb1} + \text{Clb2}) : (\text{Clb5} + \text{Clb6}) : (\text{Sic1} + \text{Cdc6}) =$$
$$(0.6 + 2.4) : (0.6 + 0.6) : (1 + ?) : (1.5 + ?) = 3 : 1.2 : 1^{+} : 1.5^{+} \ .$$

All variables are expressed in arbitrary units (au) that have been scaled so that the variables are dimensionless numbers of order 1. If desirable or necessary, it is possible to retrieve the units of most variables given some additional information. For example, the volume (mass) of a dividing (wild-type, diploid) yeast cell is ~150 fL (150 pg), see Figure 6A of (22). Hence, 1 au of the "size" variable in our model (V = 2.37 au at division; see Figure 2) corresponds to a volume of 60 fL or a mass of 60 pg per diploid cell (30 fL and 30 pg per haploid cell). In like manner, the average value of [Clb5] over one cycle is 0.098 au in our model, which corresponds to ~900 molecules per diploid cell (22), so 0.1 au of [Clb5] is 900 molec/100 fL. Hence, 1 au of [Clb5] is ~90 molec/fL = 15 nM. The same estimate holds true for Clb2, Cln2 and CKI.

Determination of Mutant Phenotype

We introduce the following rules to determine whether a given mutant phenotype is "viable" or "inviable". For a simulated cell to be viable, it must execute the following events in order: origin

relicensing ([ORI] reset to zero at the beginning of each new cell cycle); origin activation (due to a subsequent rise in [Clb5] and/or [Clb2], causing [ORI] to increase above 1); spindle alignment (due to a rise in [Clb2], causing [SPN] to increase above 1); cleavage of cohesin rings (the [Esp1] variable going through θ_{cleave}); and finally [Clb2] dropping below a threshold θ_{cd} to trigger cell division. If these events do not occur in this order, the simulated cell is considered inviable. If division occurs in an "unbudded cell" (i.e., when [BUD] <1), this also is considered inviable. Last, if cell mass ever exceeds 10, the cell is considered inviable.

For viable strains, we record cell size relative to wild-type at the time of division. Inviable strains are classified according to their failure to execute a certain event. Failure to activate origins of replication is classified as G1 arrest; e.g., *cln1Δ cln2Δ cln3Δ* cells (Figure S1A). Due to high levels of Cdh1 and CKI in this mutant, Clb2 and Clb5 are inhibited and consequently [ORI] remains close to zero. Figure S1 also illustrates metaphase- and telophase-arrested phenotypes: (panel B) the *cdc20Δ* strain enters M phase but Clb2 level goes so high that Cdc14 cannot be released from the nucleolus; (panel C) the *cln1Δ cln2Δ cln3Δ cdh1Δ* strain arrests in telophase because Clb2 never drops below θ_{cd}, even though Cdc14 is released from the nucleolus.

Simulation and Parameterization

The system of ODEs in Table S2 was solved using PET and Virtual Cell software, which are freely available on the web (both packages are suitable for simulating our model). We estimated all parameter values in the model (Table S3) by fitting simulation results to the experimentally observed phenotypes of 263 mutant strains of budding yeast (see Table S4, whose 293 entries include predicted phenotypes of 30 additional strains). All mutants in Table S4 were simulated by combining the alleles listed in Table S5, where we describe the parameter changes used to simulate each allele.

We used two criteria for fitting parameter values to this data set: (a) to maximize the number of correctly simulated mutant phenotypes, and (b) to give priority to mutant strains with well-characterized phenotypes that have been independently confirmed. For example, the phenotype of the *CLB1 clb2Δ pds1Δ* strain has been reported in only one publication (25), and its phenotype differs from that predicted by our model and all other models (11, 13). It is possible, of course, to find many parameter sets that are consistent with the phenotype of this strain, but they are all inconsistent either with many other observations or with the phenotype of a "high priority" strain. Hence, we choose to tolerate the wrong phenotype of the *CLB1 clb2Δ pds1Δ* strain in order to maximize the correct phenotypes of many other well-characterized strains.

The "basal" parameter set reported in Table S3 is the best set we have found so far by a manual search of parameter space, guided by PET and the two criteria above. We have tried a number of optimization strategies for searching the parameter space automatically, see e.g. (26, 27), but they have not found any parameter sets that are significantly better. The basal parameter set accounts for the observed phenotypes of 98% of the strains in the tests set (the six strains that are

not correctly simulated are indicated in red in Table S4). The basal parameter set is not "optimal" in any rigorous sense; it's just "quite good".

Only the rate constants for protein synthesis and degradation refer to actual biochemical reactions. The γ parameters in Type-2 equations estimate the effective time-scales on which post-translational modifications seem to occur, but the ω parameters are purely phenomenological. Their values determine how competing enzymes (e.g., kinases and phosphatases) vie for dominance over a phosphorylated substrate, but they have no direct biochemical meaning.

In general, mutant phenotypes are not super-sensitive to parameter values (1 or 2 significant figures are sufficient). Nonetheless, some parameter values are given to 4 or 5 significant figures in Table S3. Such seeming precision is partly an historical accident of how the parameter values were determined, and partly a reflection of the fact that the phenotypes of a few strains are very sensitive to specific parameter values. For example, the strains *cln1Δ cln2Δ cdh1Δ* (viable) and *cln1Δ cln2Δ cln3Δ cdh1Δ* (telophase arrest) are quite sensitive to $k_{s,cki,swi5}$ and $k_{s,clb2,m1}$. For a 2% increase in $k_{s,cki,swi5}$ or a 1.4% decrease in $k_{s,clb2,m1}$, the two mutant strains behave as observed, but a 9% increase to $k_{s,cki,swi5}$ (or a 4% decrease to $k_{s,clb2,m1}$) is already a problem for *cln1Δ cln2Δ cln3Δ cdh1Δ* cells, which divide after the first cycle and arrest in telophase only in the second cycle. On the other hand, increasing $k_{s,clb2,m1}$ to 0.2 (+1% change) changes the phenotype of *cln1Δ cln2Δ cdh1Δ* cells, which eventually (after five cycles) arrest in telophase. Were it not for the viability of *cln1Δ cln2Δ cdh1Δ* cells, we could find a parameter set for which *cln1Δ cln2Δ cln3Δ cdh1Δ* cells robustly arrest in telophase.

Over-fitting or Over-determination?

Granted that the parameters in our model are phenomenological descriptors of complex underlying biochemistry, what basis do we have to believe that the "basal" set of parameter values in Table S3 are reflective at all of the "true" state of affairs in budding yeast cells? The model has ~140 parameters that need to be estimated from the data (the qualitative phenotypes of 263 mutant yeast strains plus a few pieces of quantitative information from literature). The parameters are spread more-or-less evenly across the 29 genes comprising the network. For each gene, we have information on a gene-deletion mutant, and for many we have overexpression mutants. Each mutant provides at least one independent piece of information (viable; inviable) and usually more (size at division; phase of arrest). Double-, triple- and quadruple mutants provide additional information, especially about parameters that specify the interactions among different gene products. It is reasonable to assume that the number of independent pieces of experimental evidence from the data set of mutant phenotypes is considerably larger than the 140 parameter values that need to be estimated from the data. Even though the data is mostly "qualitative", the sheer magnitude of the information provides effective constraints on the parameters. In our experience, when we apply automatic parameter optimization algorithms (both deterministic and stochastic) to models of this sort, we do not find parameter sets that do

much better than hand-crafted sets, nor do we find alternative parameter sets that do even as well.

Hence, we believe that the model is not "over-fitting" the data, and its success in accounting for the observed phenotypes of so many different cell cycle mutants must be viewed as confirmation of the essential accuracy of the underlying mechanism and efficacy of the modeling approach. The fact that 2% of the mutant strains are not correctly simulated indicates that there are still unresolved discrepancies between the data and our present understanding of the control mechanism.

Over-determination of the data is a separate issue and more difficult to address. It could well be that a particular mutant is inviable not for the reason ascribed to it by our model, but for an entirely different reason that is not considered in our underlying mechanism. That is, the model might have enough flexibility to account for mutant phenotypes for reasons completely unrelated to the real underlying cause. Such situations can be identified only as new information appears to distinguish among alternative causes.

3. Simulation of START Mutants

The phenotypes of all START mutant strains that are discussed in the main text of the manuscript are described in Table S6.

SSA1 and YDJ1 Mutants

In early G1 phase, Cln3 is sequestered to the endoplasmic reticulum (ER) by binding to Ssa1. Later in G1, Ydj1 binds to Ssa1, displacing Cln3 from the ER and allowing Cln3:Cdk1 to enter the nucleus, where it triggers the START transition (3). In G2/M phase, Clb2:Cdk1 phosphorylates Ssa1, releasing it from Ydj1 and allowing Ssa1P to bind to Cln3 and draw it back to the ER. For this reason, Cln3:Cdk1 is active in the nucleus between late G1 and early M in our simulations, as observed experimentally (28). Cells lacking the *SSA1* gene are viable and approximately 85% of the wild-type cell size (29), whereas cells lacking the *YDJ1* gene are viable and 1.85 times larger than wild-type cells (30), see Supplemental Table S6.

Rescue of the Inviable Triple-cln Deletion Strain

As discussed in the main text of the manuscript, the deletion of the *SIC1* gene rescues the triple-*cln* deletion strain but is not sufficient to rescue *cln3Δ bck2Δ* cells. Figure S2 illustrates that, compared to triple-*cln* deletion cells, *cln3Δ bck2Δ sic1Δ* cells have significantly lower levels of Clb5,6 cyclins as well as low levels of Cln1,2 cyclins. Hence, *cln3Δ bck2Δ sic1Δ* cells are unable to inactivate APC:Cdh1.

4. Simulation of FINISH Mutants

The phenotypes of all FINISH mutant strains that are discussed in the main text of the manuscript are described in Table S7.

Cdc14 Oscillations

Cdc14 "endocycles" are a consequence of a negative feedback loop in the MEN (Cdc5 ⊣ Net1 ⊣ Cdc14 → Cdh1 ⊣ Cdc5), as demonstrated by simple mathematical (31-33). To test this hypothesis, we have used the model to ask whether Cdc14 endocycles are likely to be observed in strains carrying the *GAL-CLB2-dbΔ* gene in combination with mutant alleles of other genes. Simulations show that Cdc14 endocycles persist in *GAL-CLB2-dbΔ cdc15^{as1}*, *GAL-CLB2-dbΔ swi5Δ*, *GAL-CLB2-dbΔ cdc20-3*, *GAL-CLB2-dbΔ pds1Δ cdc20Δ clb5Δ* mutants (Figure S3A,B,C,D), but they are absent in *GAL-CLB2-dbΔ cdc5-1*, *GAL-CLB2-dbΔ CDC5-dbΔ, GAL-CLB2-dbΔ cdh1Δ,* and *GAL-CLB2-dbΔ cdc14-1* mutants (Figure S4A,B,C,D).

Blocking the Transcriptional Regulatory Network

Recently it has been observed that the synthesis of many proteins, including some cell cycle proteins, remains on schedule in budding yeast strains lacking all *CLB* genes (34, 35). These authors have proposed (34, 36) that a transcriptional regulatory network plays a substantial or even a major role in regulating progression through the budding yeast cell cycle. Using our model, we have tested whether cells with constitutive gene expression can exhibit normal cell cycle progression. Our model predicts normal cycling in a mutant strain (*mbp1*Δ *mcm1*Δ *swi4*Δ *swi5*Δ *swi6*Δ *GAL-CLB2 GAL-CDC5 GAL-CDC20 GAL-CLN2*(low) *GAL-SIC1*(low)) in which all genes regulated by transcription factors are replaced by constitutive production. However, viability of this strain is very sensitive to synthesis rates and other parameters, as will be demonstrated in the following section.

5. Robustness Analysis of Predicted Phenotypes

The model we have described so far (the equations in Table S2 + the basal parameter set in Table S3 + the prescriptions for simulating mutant alleles in Table S5) is successful in explaining the phenotypes of 98% of experimentally characterized mutant strains in our collection (Table S4). There are several possible reasons for the 2% inconsistencies that remain between the model and the data set. It may be that there exists a region of parameter space that does a better job, but we have just not found it yet. It may be that there are mistakes in the wiring diagram that render the model unable to explain certain facts, regardless of how parameter values are chosen. It may be that some reported phenotypes are incorrect or mistakenly interpreted.

In light of these realities, how should we use the model to predict the phenotypes of novel combinations of mutant alleles? The model has 29 different genes that may be mutated in a variety of ways: gene deletion, overexpression, temperature-sensitive alleles, non-

phosphorylable sites, constitutive phospho-mimics, destruction-box deletion, etc. The number of possible combinations of five genes with 78 alleles (listed in the Table S5) each exceeds 20×10^6. Only a small fraction of all possible combinations of mutant alleles of cell cycle genes in budding yeast have actually been characterized experimentally, and it is practical to test only a tiny fraction of all possible predictions that could be made by the model. In Table S8 we list the predictions we have made so far in this paper, using the basal set of parameter values (Table S3).

Can we assign a confidence measure to such predictions? Because the basal parameter set is not necessarily the "correct" set, we should not base our predictions on the singular, basal set of parameter values. We would like to have a collection of "acceptable" sets of parameters values, on which we could make a range of predictions and classify the predictions as "robust" (insensitive to parameter values) or "fragile" (sensitive to parameter values). The problem with this approach is that we have many parameter values to assign (133 adjustable parameters in Table S3) on the basis of the observed phenotypes of many mutant strains (263 mutant strains in Table S4). It is impossible to search thoroughly a 133-dimensional parameter space for parameter vectors that satisfy the constraints imposed by 263 mutant phenotypes. In order to get started on such a robustness analysis, we must make some compromises.

For this manuscript we have chosen to focus on the 12 mutant strains listed in Table 1 (main text). First, we predicted the phenotypes of these strains based on the basal parameter set in Table S3. Next, we made a range of predictions based on alternative parameter sets that are consistent with a subset of the mutant strains in Table S4. As our "bench-mark" strains, we chose only mutant strains with single gene deletions, because the phenotypes of these strains are very well characterized. We introduced random perturbations (±30%) of all parameters simultaneously, and we retained only those parameter sets that are consistent with the phenotypes of the bench-mark strains. To get a sample of 1000 alternative parameter sets that are acceptable by this criterion, we had to simulate more than 10^5 potential parameter sets.

We used these alternative parameters sets to measure how frequently the phenotype ("viable" or "inviable") predicted by the basal parameter set is corroborated by the alternative parameter sets, for each of the mutant strains in Table 1. The histogram in Figure S5 displays the results of this robustness analysis. The frequency of "phenotype change" is defined as $f = 1 - (N_r/N_{total})$, where N_r is the number of times an alternative parameter set reproduces the predicted phenotype of the basal parameter set, and $N_{total} = 1000$ is the total number of alternative parameter sets. The histogram in Figure S5 suggests that there are two distinct groups of predictions of mutant phenotypes roughly separated by the average value of f ($f_{av} = 0.3$). Indeed if the mutant strains are separated into two groups with $f < f_{av}$ and $f > f_{av}$, then these groups form two statistically distinct distributions. (The Student T-test for these two distributions gives p-value = 0.0014, well below the usual significance level of 0.05.) The predictions we make of these two groups of mutant strains we describe as "robust" ($f < f_{av}$) and "fragile" ($f > f_{av}$). Robust predictions are insensitive to values of fitting parameters; fragile predictions are very sensitive. Robust phenotypes evidently emerge from the regulatory network itself; hence, future experimental tests

of robust predictions will either confirm the underlying control system or shed light on new regulatory mechanisms for the cell division cycle. On the other hand, future experimental tests of fragile predictions will help to constrain adjustable parameters of the model.

For some mutant strains we expect that predictions of a deterministic model will be fragile because the phenotype of some mutant strains is inherently stochastic or sensitive to environmental conditions such as temperature or growth rate. For example *lte1Δ* is known to be cold sensitive (37), *cdc14Δ GAL-SIC1* is reported to be partially viable (38), and *CLB2-dbΔ clb5Δ* is viable in galactose and inviable in glucose (39). The phenotypes of these mutants are "fragile in nature" and robustness analysis also shows that phenotypes of these three strains are sensitive to parameter perturbations (f = 0.44, 0.62 and 0.91, respectively). Another example is the double mutant *cdc20Δ pds1Δ*. In our robustness analysis, this mutant strain changes phenotype (from inviable to viable) in 59% of tested parameter sets. For comparison, f = 1% for *cdc20Δ* strain. Thus, the phenotype of *cdc20Δ pds1Δ* is fragile (very sensitive to parameter perturbations) compared to *cdc20Δ*. As discussed above, the lethality of *cdc20Δ pds1Δ* can be rescued either by deleting *CLB5* or by adding multiple copies of *SIC1*. Therefore, a high frequency of phenotype change for an inviable strain mutant may indicate that the strain can be rescued by deletion or overexpression of other genes in the network.

6. Experimental Validation of Predictions

Three strains in Table 1, though not included among our 263 test strains, were previously characterized in publications, and their observed phenotypes matched our predictions. Two novel strains in Table 1 were constructed by our collaborators (40). As predicted, *cln1*Δ *cln2*Δ *mbp1*Δ cells are viable, which is a sensitive test of our estimate that the rate constants for Clb5,6 synthesis driven by SBF (the Swi6:Swi4 complex) and by MBF (the Swi6:Mbp1 complex) are comparable. If the SBF-driven rate of synthesis of Clb5,6 were much smaller than the MBF-driven rate, then *cln1*Δ *cln2*Δ *mbp1*Δ would be predicted to have the same inviable phenotype as *cln1*Δ *cln2*Δ *swi4*Δ, because *cln1*Δ *cln2*Δ *clb5*Δ *clb6*Δ is also observed to be inviable (41).

Contrary to the robust prediction that *cln3*Δ *swi4*Δ *whi5*Δ cells are dead, they are viable and large (~3.4× wild-type size at division) (40). According to our assumptions, Whi5 binds to and inhibits only Swi4:Swi6 dimers (SBF) and not Swi6:Mbp1 dimers (MBF). Hence, the phenotypes of the *cln3*Δ *swi4*Δ and *cln3*Δ *swi4*Δ *whi5*Δ strains should be identical (inviable). The viability of *cln3*Δ *swi4*Δ *whi5*Δ cells suggests that Whi5 plays some role in inhibiting MBF, contrary to the evidence from co-immunoprecipitation studies (42, 43).

7. Incorrectly simulated mutant strains

In this section we discuss the six incorrectly simulated mutant strains marked in red in Table S4. Four of these strains (*sic1*Δ *GAL-CLB2, cdh1*Δ *GAL-CLB2, swi5*Δ *GAL-CLB2* and *APC-A GAL-CLB2*) overexpress Clb2 protein and must be evaluated relative to the *GAL-CLB2* control strain,

which is viable. Strains that overexpress Clb2 have a long G1 phase, because Clb2-dependent kinase inhibits both SBF and MBF in our model. For the *GAL-CLB2* strain to be viable, we must limit the total expression of Clb2 in order that the cells may successfully bud. This level of overexpression of Clb2 is insufficient to cause telophase arrest, which is reported to be the terminal phenotype of *sic1*Δ *GAL-CLB2* and *swi5*Δ *GAL-CLB2* (44), although convincing evidence is not shown. On the other hand *cdh1*Δ *GAL-CLB2* cells are reported (39) to arrest as a mixture of predominantly unbudded cells and some large budded cells, suggesting a budding defect in this strain. In our model, for levels of Clb2 that are consistent with the viability of the *GAL-CLB2* strain, the four double-mutant strains are inviable because of budding defects. Because the experimental evidence is sketchy, it is not clear whether our simulations of these four Clb2-overexpressing strains are correct or incorrect.

Similarly, the high level of Cln2 in the *cln1*Δ *cln2*Δ *cdh1*Δ *GAL-CLN2* strain results in an unrealistically small cell size and short G1 phase, indicating that there are other limits on G1 progression that are not taken into account in our model. The model does not include repressors, such as Nrm1 and Yox1, which are degraded by Cdh1 and thus can affect G1 progression in the *cln1*Δ *cln2*Δ *cdh1*Δ *GAL-CLN2* strain.

Very little is known about the *clb2*Δ *CLB1 pds1*Δ strain, which is reportedly inviable (25). However, our model predicts that it should be viable.

As described in the Mathematical Model section, we model protein phosphorylation and complex formation using "soft" and "hard" Heaviside functions, respectively. This approach has drawbacks when modeling overexpression of a protein that is involved in a complex, when the rate-limiting step (phosphorylation) follows the fast complex formation. If an abundant protein forms a complex with another protein and this complex is subsequently phosphorylated (a slower reaction), then, in our modeling formalism, the total amount of phosphorylated complex is insensitive to an increase in the abundant protein. However, in $WHI5^{OP}$ cells the rate of Whi5 phosphorylation in the Swi4:Swi6:Whi5 complex must be less than in wild type cells because more time is required for cyclin-dependent kinases to phosphorylate the excess of Whi5 in the overexpressing cells. This effect is important to account for the delay of START and the large size of $WHI5^{OP}$ cells compared to wild-type cells. However, in our modeling approach, the increase of total Whi5 does not change the amount of the complex and has no explicit impact on the rate of phosphorylation of Whi5 in the Swi4:Swi6:Whi5 complex. To model this mutant, we reduce the phosphorylation rate of Swi4:Swi6:Whi5 by a factor of the excess of Whi5 over its wild-type level. We use the same approach for simulating *GAL-NET1* strains. In this way we keep the modeling approach simple and yet describe overproduction of species involved in complex formation and phosphorylation reactions.

References:

1. Hartwell LH, Culotti J, Pringle JR, Reid BJ. Genetic control of the cell division cycle in yeast. Science. 1974;183:46-51.
2. Enserink JM, Kolodner RD. An overview of Cdk1-controlled targets and processes. Cell Division. 2010;5:11-52.
3. Verges E, Colomina N, Gari E, Gallego C, Aldea M. Cyclin Cln3 is retained at the ER and released by the J chaperone Ydj1 to trigger cell cycle entry. Mol Cell. 2007;26:649-62.
4. de Bruin RAM, McDonald WH, Kalashnikova TI, Yates J, III, Wittenberg C. Cln3 activates G1-specific transcription via phosphorylation of the SBF bound repressor Whi5. Cell. 2004;117:887-98.
5. Costanzo M, Nishikawa JL, Tang X, Millman JS, Schub O, Breitkreuz K, et al. CDK activity antagonizes Whi5, an inhibitor of G1/S transcription in yeast. Cell. 2004;117:899-913.
6. Wijnen H, Landman A, Futcher B. The G1 cyclin Cln3 promotes cell cycle entry via the transcription factor Swi6. Mol Cell Biol. 2002;22:4402-18.
7. Charvin G, Oikonomou C, Siggia ED, Cross FR. Origin of irreversibility of cell cycle start in budding yeast. PL0S Biol. 2010;8:e1000284.
8. Dirick L, Nasmyth K. Positive feedback in the activation of G1 cyclins in yeast. Nature. 1991;351(June 27):754-7.
9. Nasmyth K. Control of the yeast cell cycle by Cdc28 protein kinase. Curr Opin Cell Biol. 1993;5:166-79.
10. Koch C, Schleiffer A, Ammerer G, Nasmyth K. Switching transcription on and off during the yeast cell cycle: Cln/Cdc28 kinases activate bound transcription factor SBF (Swi4/Swi6) at Start, whereas Clb/Cdc28 kinase displace it from the promoter in G2. Genes Dev. 1996;10:129-41.
11. Chen KC, Calzone L, Csikasz-Nagy A, Cross FR, Novak B, Tyson JJ. Integrative analysis of cell cycle control in budding yeast. Mol Biol Cell. 2004;15:3841-62.
12. Marlovits G, Tyson CJ, Novak B, Tyson JJ. Modeling M-phase control in *Xenopus* oocyte extracts: the surveillance mechanism for unreplicated DNA. Biophys Chem. 1998;72:169-84.
13. Laomettachit T, Chen KC, Baumann WT, Tyson JJ. Modeling Protein Regulatory Networks Using Standardized Components with Application to the START Transition in the Budding Yeast Cell Cycle. in submission. 2015.
14. Mjolsness E, Sharp DH, Reinitz J. A connectionist model of development. J Theor Biol. 1991;152(4):429-53.
15. Molinelli EJ, Korkut A, Wang W, Miller ML, Gauthier NP, Jing X. Perturbation Biology: Inferring Signaling Networks in Cellular Systems. PLoS Comput Biol 2013;9(12):e1003290.
16. Singhania R, Sramkoski RM, Jacobberger JW, Tyson JJ. A hybrid model of mammalian cell cycle regulation. PLoS Comput Biol. 2011;7(2):e1001077.
17. Glass L, Kauffman S. The logical analysis of continuous non-linear biochemical control networks. J Theor Biol. 1973;39:103–29.
18. Li F, Long T, Lu Y, Ouyang Q, Tang C. The yeast cell-cycle network is robustly designed. Proc Natl Acad Sci USA. 2004;101:4781-6.
19. Poirel CL, Rodrigues RR, Chen KC, Tyson JJ, Murali TM. Top-down network analysis to drive bottom-up modeling of physiological processes. J Comput Biol. 2013;20:409-18.
20. Rock JM, Amon A. Cdc15 integrates Tem1 GTP-ase mediated spatical signals with Polo kinase-mediated temporal cues to activate mitotic exit. Genes Dev. 2012;25:1943-54.
21. Chen KC, Csikasz-Nagy A, Gyorffy B, Val J, Novak B, Tyson JJ. Kinetic analysis of a molecular model of the budding yeast cell cycle. Mol Biol Cell. 2000;11:369-91.
22. Cross FR, Archambault V, Miller M, Klovstad M. Testing a mathematical model for the yeast cell cycle. Mol Biol Cell. 2002;13:52-70.

23. Archambault V, Li CX, Tackett AJ, Wasch R, Chait BT, Rout MP, et al. Genetic and biochemical evaluation of the importance of Cdc6 in regulating mitotic exit. Mol Biol Cell. 2003;14:4592-604.
24. Ghaemmaghami S, Huh W-K, Bower K, Howson RW, Belle A, Dephoure N, et al. Global analysis of protein expression in yeast. Nature. 2003;425:737-41.
25. Shirayama M, Toth A, Galova M, Nasmyth K. APC (CDC20) promotes exit from mitosis by destroying the anaphase inhibitor Pds1 and cyclin Clb5. Nature. 1999;402:203-7.
26. Oguz C, Teeraphan L, Chen KC, Watson LT, Baumann WT, Tyson JJ. Optimization and model reduction in the high dimensional parameter space of a budding yeast cell cycle model. BMC Systems Biology. 2013;7:53.
27. Andrew TM, Amos BD, Easterling DR, Oguz C, Baumann WT, Tyson JJ, et al. Global Parameter Estimation for a Eukaryotic Cell Cycle Model in Systems Biology. Proceeding SummerSim '14 Proceedings of the 2014 Summer Simulation Multiconference. 2014.
28. Truman AW, Kristjansdottir K, Wolfgeher D, Hasin N, Polier S, Zhang H, et al. CDK-dependent Hsp70 phosphorylation controls G1 cyclin abundance and cell cycle progression. Cell. 2012;151:1308-18.
29. Burtner CR, Murakami C, J. Olsen B, Kennedy BK, Kaeberlein M. A genomic analysis of chronological longevity factors in budding yeast. Cell Cycle. 2011;10(9):1385-96.
30. Jorgensen P, Nishikawa JL, Breitkreutz B-J, Tyers M. Systematic identification of pathways that couple cell growth and division in yeast. Science. 2002;297:395-400.
31. Manzoni R, Visintin C, Montani F, Ciliberto A, Visintin R. Oscillation in Cdc14 release and sequestration reveal a circuit underlying mitotic exit. J Cell Biol. 2010;180:210-22.
32. Vinod PK, Freire P, Rattani A, Ciliberto A, Uhlmann F, Novak B. Computational modeling of mitotic exit in budding yeast; the role of separase and Cdc14 endocycles. J R Soc Interface. 2011;8:1128-41.
33. Lu Y, Cross FR. Periodic cyclin-Cdk activity entrains an autonomous Cdc14 release oscillator. Cell. 2010;141:268-79.
34. Kovacs LAS, Orlando DA, Haase SB. Transcription networks and cyclin/CDKs: The yin and yang of cell cycle oscillators Cell Cycle. 2008;7:2626-9.
35. Kovacs LAS, Mayhew MB, Orlando DA, Jin Y, Li Q, Huang C, et al. Cyclin-dependent kinases are regulators and effectors of oscillations driven by a transcription factor network. Mol Cell. 2012;45:669–79.
36. Bristow SL, Leman AR, Simmons Kovacs LA, Deckard A, Harer J, Haase SB. Checkpoints couple transcription network oscillator dynamics to cell-cycle progression. Genome Biology. 2014;15(9).
37. Zhao X, Chang AY, Toh-E A, Arvan P. A role for Lte1p (a low temperature essential protein involved in mitosis) in proprotein processing in the yeast secretory pathway. J Biol Chem 2007;282(3):1670-8.
38. Jaspersen SL, Charles JF, Tinker-Kulberg RL, Morgan DO. A late mitotic regulatory network controlling cyclin destruction in *Saccharomyces cerevisiae*. Mol Biol Cell. 1998;9:2803-17.
39. Cross FR. Two redundant oscillatory mechanisms in the yeast cell cycle. Dev Cell. 2003;4:741-52.
40. Adames N, Peccoud J. private communication.
41. Schwob E, Nasmyth K. *CLB5* and *CLB6*, a new pair of B cyclins involved in DNA replication in *Saccharomyces cerevisiae*. Genes Dev. 1993;7:1160-75.
42. Harris MR, Lee D, Farmer S, Lowndes NF, De Bruin RAM. Binding specificity of the G1/S transcriptional regulators in budding yeast. PLoS One. 2013;8:e61059.
43. Travesa A, Kalashnikova TI, de Bruin RAM, Cass SR, Chahwan C, Lee DE, et al. Repression of G1/S transcription is mediated via interaction of the GTB motifs of Nrm1 and Whi5 with Swi6. Mol Biol Cell. 2013;33(8):1476-86.

44. Toyn JH, Johnson AL, Donovan JD, Toone WM, Johnston LH. The Swi5 transcription factor of *Saccharomyces cerevisiae* has a role in exit from mitosis through induction of the cdk-inhibitor Sic1 in telophase. Genetics. 1997;145:85-96.
45. de Bruin RAM, Kalashnikova TI, Chahwan C, McDonald WH, Wohlschlegel J, Yates JI, et al. Constraining G1-specific transcription to late G1 phase: the MPF associated corepressor Nrm1 acts via negative feedback. Mol Cell. 2006;23:483-96.
46. Koch C, Moll T, Neuberg M, Ahorn H, Nasmyth K. A role for the transcription factors Mbp1 and Swi4 in progression from G1 to S phase. Science. 1993;261:1551-7.
47. Ferrezuelo F, Aldea M, Futcher B. Bck2 is a phase-independent activator of cell cycle-regulated genes in yeast. Cell Cycle. 2009;8:239-52.
48. Wijnen H, Futcher B. Genetic analysis of the shared role of *CLN3* and *BCK2* at the G_1-S transition in *Saccharomyces cerevisiae*. Genetics. 1999;153:1131-43.
49. Richardson HE, Wittenberg C, Cross F, Reed SI. An essential G1 function for cyclin-like proteins in yeast. Cell. 1989;59(December 22):1127-33.
50. Tyers M. The cyclin-dependent kinase inhibitor $p40^{sic1}$ imposes the requirement for Cln G1 cyclin function at Start. Proc Natl Acad Sci USA. 1996;93:7772-6.
51. Schneider BL, Yang Q-H, Futcher AB. Linkage of replication to Start by the Cdk inhibitor Sic1. Science. 1996;272:560-2.
52. Epstein CB, Cross FR. *CLB5*: a novel B cyclin from budding yeast with a role in S phase. Genes Dev. 1992;6:1695-706.
53. Schwab M, Lutum AS, Seufert W. Yeast Hct1 is a regulator of Clb2 cyclin proteolysis. Cell. 1997;90:683-93.
54. Dirick L, Bohm T, Nasmyth K. Roles and regulation of Cln/Cdc28 kinases at the start of the cell cycle of *Saccharomyces cerevisiae*. EMBO J. 1995;14:4803-13.
55. Flick K, Wittenberg C. Multiple pathways for suppression of mutants affecting G1-specific transcription in *Saccharomyces cerevisiae*. Genetics. 2005;169(1):37-49.
56. Nasmyth K, Dirick L. The Role of *SWI*4 and *SWI*6 in the activity of G1 cyclins in yeast. Cell. 1991;66(September 6):995-1013.
57. Visintin R, Craig K, Hwang ES, Prinz S, Tyers M, Amon A. The phosphatase Cdc14 triggers mitotic exit by reversal of Cdk-dependent phosphorylation. Mol Cell. 1998;2:709-18.
58. Yamamoto A, Guacci V, Koshland D. Pds1p, an inhibitor of anaphase in budding yeast, plays a critical role in the APC and checkpoint pathway(s). J Cell Biol. 1996;133:99-110.
59. Wang Y, Burke DJ. Cdc55p, the B-type regulatory subunit of protein phosphatase 2A, has multiple functions in mitosis and is required for the kinetochore/spindle checkpoint in *Saccharomyces cerevisiae*. Mol Cell Biol. 1997;17:620-6.
60. Lim HH, Goh P-Y, Surana U. Cdc20 is essential for the cyclosome-mediated proteolysis of both Pds1 and Clb2 during M phase in budding yeast. Curr Biol. 1998;8:231-4.
61. Thornton BR, Toczyski DP. Securin and B-cyclin/CDK are the only essential targets of the APC. Nat Cell Biol. 2003;5:1090-4.
62. Geymonat M, Jensen S, Johnston LH. Mitotic exit: the Cdc14 double cross. Current Biology. 2002;12:R482–R4.
63. Cohen-Fix O, Peters J-M, Kirschner MW, Koshland D. Anaphase initiation in Saccharomyces cerevisiae is controlled by the APC-dependent degradation of the anaphase inhibitor Pds1p. Genes Dev. 1996;10:3081-93.
64. Stegmeier F, Visintin R, Amon A. Separase, polo kinase, the kinetochore protein Slk19, and Spo12 function in a network that controls Cdc14 localization during early anaphase. Cell. 2002;108:207-20.
65. Lu Y, Cross FR. Mitotic exit in the absence of separase activity. Mol Biol Cell. 2009;20:1576-91.

66. Alexandru G, Zachariae W, Schleiffer A, Nasmyth K. Sister chromatid separation and chromosome reduplication are regulated by different mechanisms in response to spindle damage. EMBO J. 1999;18:2707-21.
67. Shirayama M, Matsui Y, Toh-e A. The yeast TEM1 gene, which encodes a GTP-binding protein, is involved in termination of M phase. Mol Cell Biol. 1994;14:7476-82.
68. Visintin R, Hwang ES, Amon A. Cfi1 prevents premature exit from mitosis by anchoring Cdc14 phosphatase in the nucleolus. Nature. 1999;398:818-23.
69. Shou W, Deshaies RJ. Multiple *telophase arrest bypassed (tab)* mutants alleviate the essential requirement for Cdc15 in exit from mitosis in *S. cerevisiae*. BMC Genetics. 2002;3:4.
70. Hu F, Wang Y, Liu D, Li Y, Qin J, Elledge S. Regulation of the Bub2/Bfa1 GAP complex by Cdc5 and cell cycle checkpoints. Cell. 2001;107:655-65.
71. Sopko R, Huang D, Preston N, Chua G, Papp B, Kafadar K, et al. Mapping pathways and phenotypes by systematic gene overexpression. Mol Cell. 2006;21(3):319-30.
72. Sullivan M, Uhlmann F. A non-proteolytic function of separase links the onset of anaphase to mitotic exit. Nature Cell Biol. 2003;5:249-54.
73. Visintin C, Tomson BN, Rahal R, Paulson J, Cohen M, Tauton J, et al. APC/Cdh1 mediated degradation of the polo kinase Cdc5 promotes the return of Cdc14 into the nucleolus. Genes Devel. 2008;22:79-90.
74. Visintin R, Stegmeier F, Amon A. The role of the polo kinase Cdc5 in controlling Cdc14 localization. Mol Biol Cell. 2003;14:4486-98.

Table S1. Variables and initial values.

Variable*	Description	Eq#	Class	Initial Value
[APCP]	Active (phosphorylated) form of APC	(40)	2	1.137
$[Bck2_T]$	Total concentration of Bck2	(8)	1	0.2698
$[Bub2_A]$	Bfa1:Bub2, inhibitor of Tem1	(57)	2	0.024
[BUD]	Progress to bud emergence	(25)	1	0.03
$[Cdc5_A]$	Active form of Cdc5 polo-like kinase	(56)	2	0.5
$[Cdc5_T]$	Total Cdc5 polo-like kinase	(55)	1	0.272
[Cdc14c]	Cytoplasmic Cdc14 phosphatase	(52)	3	0
[Cdc14n]	Cdc14 located in cell nucleus	(54)	3	1.725
[Cdc14]	Active form of Cdc14 which is total free Cdc14	(53)	3	1.725
$[Cdc15_A]$	Active form of Cdc15 kinase	(59)	2	0.86
$[Cdc15_{AF}]$	Active form that is not in a complex with Tem1	(51)	3	0.34
$[Cdc20_T]$	Total Cdc20, an APC partner	(42)	1	0.599
$[Cdc20_A]$	Total active form of Cdc20	(43)	3	0.536
$[Cdc20_A : APC]$	Active form of Cdc20:APC complex	(45)	3	0
$[Cdc20_A : APCP]$	Active form of Cdc20:APCP complex	(44)	3	0.536
$[Cdc55_A]$	Active form of Cdc55 phosphatase	(49)	2	0.027
$[Cdh1_A]$	Active form of Cdh1, an APC partner	(38)	2	0.787
[CKIP]	Phosphorylated forms of Sic1 & Cdc6	(29)	2	8.645
$[CKI_T]$	Total cyclin inhibitors Sic1 & Cdc6	(28)	1	0.0218
[Clb2]	Active forms of cyclins Clb1 & Clb2	(32)	2	0.157
$[Clb2_T]$	Total cyclins Clb1 & Clb2	(27)	1	0.1747
$[Clb2_F]$	cyclins Clb1 & Clb2 free from CKI	(31)	3	0.157
[Clb5]	Active forms of cyclins Clb5 & Clb6	(30)	3	0.034
$[Clb5_T]$	Total cyclins Clb5 & Clb6	(26)	1	0.038
[Cln2]	Total cyclins Cln1 & Cln2	(9)	1	0.196
$[Cln3_{ER}]$	Cln3 located in endoplasmic reticulum	(6)	3	0.084
$[Cln3_N]$	cyclin Cln3 located in cell nucleus	(7)	3	0

$[Cln3_T]$	Total cyclin Cln3	(5)	1	0.084
[Esp1]	Active form of separase	(48)	3	0.466
$[Mad2_A]$	Active form of spindle checkpoint protein Mad2	(41)	2	0.063
$[Mcm1_A]$	Active form of transcr factor for Clb2	(39)	2	0.21
$[Net1_A]$	Active form of inhibitor of Cdc14	(50)	2	0.2752
[ORI]	Progress to DNA synthesis	(37)	1	0.009
$[Pds1_T]$	Securin, an inhibitor of Esp1	(47)	1	0.034
$[Pr2S4_T]$	Complex between Swi4 and promoter Pr2	(17)	3	0
[Pr2S4P]	Phosphorylated forms of Swi4 bound to promoter Pr2	(16)	2	0
$[Pr2S6M1_T]$	Swi6 and Mbp1 complex bound to promoter Pr2	(19)	3	0
[Pr2S6M1P]	Phosphorylated form of Swi6 and Mbp1 complex bound to promoter Pr2	(18)	2	0
$[Pr2S6S4_T]$	Swi6 and Swi4 complex bound to promoter Pr2	(14)	3	0
[Pr2S6S4]	Non-phosphorylated form of Swi6 and Swi4 complex bound to promoter Pr2	(15)	2	0
[Pr2S6S4P]	Phosphorylated form of Swi6 and Swi4 complex bound to promoter Pr2	(13)	2	0
$[Pr2S6S4W5_T]$	Complex formed by Swi4, Swi6, Whi5 bound to promoter Pr2	(11)	3	2
[Pr2S6S4W5P]	Phosphorylated form of Swi4, Swi6 and Whi5 complex bound to promoter Pr2	(10)	2	0.136
$[Pr5S6M1_T]$	Swi6 and Mbp1 complex bound to promoter Pr5	(22)	3	1.7
[Pr5S6M1P]	Phosphorylated form of Swi6 and Mbp1 complex bound to promoter Pr5	(21)	2	0.94
$[Pr5S6S4_T]$	Swi6 and Swi4 complex bound to promoter Pr5	(24)	3	0.3
[Pr5S6S4P]	Phosphorylated form of Swi6 and Swi4 complex bound to promoter Pr5	(23)	2	0.2
$[S6M1_T]$	Complex between Swi6 and Mbp1	(20)	3	5.5
$[S6S4_T]$	Complex between Swi6 and Swi4	(12)	3	5.5
[SPN]	Progress to spindle assembly	(46)	1	0.064
$[Ssa1_F]$	Free form of Ssa1, a binding partner of Cln3 in ER	(4)	3	0.22
[Ssa1P]	Phosphorylated form of Ssa1	(3)	2	0.001
[Swe1P]	Phosphorylated form of Swe1	(34)	2	0.01
$[Swe1_T]$	Total Swe1, a negative regulator of CDK	(33)	1	0.0387
$[Swi5_A]$	Active form of Swi5	(36)	2	0.3

$[Swi5_T]$	Total Swi5, transcr factor of CKI	(35)	1	0.3
$[Tem1_A]$	Active form of Tem1, a G-protein kinase	(58)	2	0.52
$[Tem1_A : Cdc15_A]$	Complex between $Tem1_A$ and $Cdc15_A$	(60)	3	0.52
V	Cell size (in normalized volume unit)	(1)	1	1.085
[Ydj1]	J chaperone, triggers Cln3 release from ER to nucleus	(2)	1	0.78

* […] refers to normalized (dimensionless) concentration variables

Variables of class 1 describe the total concentrations of proteins that change due to protein synthesis and degradation (time scale ≈ 10 min). Class-2 variables describe post-translational modifications of proteins (e.g., phosphorylation and dephosphorylation; time scale ≈ 1 min), and class-3 variables describe the rapid formation of protein complexes (time scale ≈ 0.1 min).

Table S2. Equations of the budding yeast cell cycle model.

Cell Growth	
$\frac{dV}{dt} = \mu \cdot V \cdot \left(1 - \frac{V}{300}\right)$	(1)
START Module	
$[\text{Ydj1}] = [\text{Ydj1}_\text{T}] \cdot (1 - e^{-V/v_{\text{ydj1}}})$	(2)
$[\text{Ssa1P}] = [\text{Ssa1}_\text{T}] \cdot H(\sigma \cdot W_{\text{ssa1}})$ $W_{\text{ssa1}} = \omega_{\text{p,ssa1,b2}} \cdot [\text{Clb2}] - \omega_{\text{dp,ssa1}}$	(3)
$[\text{Ssa1}_\text{F}] = \max([\text{Ssa1}_\text{T}] - [\text{Ssa1P}] - [\text{Ydj1}], 0)$	(4)
$\frac{d[\text{Cln3}_\text{T}]}{dt} = k_{\text{s,cln3}} \cdot (1 - e^{-V/v_{\text{cln3}}}) - k_{\text{d,cln3}} \cdot [\text{Cln3}_\text{T}]$	(5)
$[\text{Cln3}_{\text{ER}}] = \min([\text{Cln3}_\text{T}], [\text{Ssa1}_\text{F}] + [\text{Ssa1P}])$	(6)
$[\text{Cln3}_\text{N}] = [\text{Cln3}_\text{T}] - [\text{Cln3}_{\text{ER}}]$	(7)
$\frac{d[\text{Bck2}_\text{T}]}{dt} = k_{\text{s,bck2}} \cdot (1 - e^{-V/v_{\text{bck2}}}) - k_{\text{d,bck2}} \cdot [\text{Bck2}_\text{T}]$	(8)
$\frac{d[\text{Cln2}]}{dt} = k_{\text{s,cln2}} + k_{\text{s,cln2,sbf}} \cdot V_{\text{S2}} - k_{\text{d,cln2}} \cdot [\text{Cln2}]$ $V_{\text{S2}} = [\text{Pr2S6S4W5P}] + [\text{Pr2S6S4P}] + e_{\text{s4s6}} \cdot [\text{Pr2S6S4}] + e_{\text{s6m}} \cdot [\text{Pr2S6M2P}] + e_{\text{s4}} \cdot [\text{Pr2S4P}]$	(9)
$\frac{d[\text{Pr2S6S4W5P}]}{dt} = \gamma \cdot ([\text{Pr2S6S4W5}_\text{T}] \cdot H(\sigma \cdot W_{\text{s6s4w5}}) - [\text{Pr2S6S4W5P}])$ $W_{\text{s6s4w5}} = \omega_{\text{a,s6s4w5,n3}} \cdot [\text{Cln3}_\text{N}] + \omega_{\text{a,s6s4w5,n2}} \cdot [\text{Cln2}] + \omega_{\text{a,s6s4w5,k2}} \cdot [\text{Bck2}_\text{T}] + \omega_{\text{a,s6s4w5,b5}} \cdot [\text{Clb5}] - \omega_{\text{i,s6s4w5}} - \omega_{\text{i,s6s4w5,b2}} \cdot [\text{Clb2}]$	(10)
$[\text{Pr2S6S4W5}_\text{T}] = \min([\text{Pr2}], [\text{S6S4}_\text{T}], [\text{Whi5}_\text{T}])$	(11)
$[\text{S6S4}_\text{T}] = \min\left([\text{Swi4}_\text{T}], [\text{Swi4}_\text{T}] \frac{[\text{Swi6}_\text{T}]}{[\text{Swi4}_\text{T}] + [\text{Mbp1}_\text{T}]}\right)$	(12)
$\frac{d[\text{Pr2S6S4P}]}{dt} = \gamma \cdot ([\text{Pr2S6S4}_\text{T}] \cdot H(\sigma \cdot W_{\text{s6s4}}) - [\text{Pr2S6S4P}])$ $W_{\text{s6s4}} = \omega_{\text{a,s6s4,n3}} \cdot [\text{Cln3}_\text{N}] + \omega_{\text{a,s6s4,n2}} \cdot [\text{Cln2}] + \omega_{\text{a,s6s4,k2}} \cdot [\text{Bck2}_\text{T}] + \omega_{\text{a,s6s4,b5}} \cdot [\text{Clb5}]$ $- \omega_{\text{i,s6s4}} - \omega_{\text{i,s6s4,b2}} \cdot [\text{Clb2}]$	(13)[1]

$[\mathrm{Pr2S6S4}_{\mathrm{T}}] = \max(0, \min([\mathrm{Pr2}], [\mathrm{S6S4}_{\mathrm{T}}]) - [\mathrm{Pr2S6S4W5}_{\mathrm{T}}])$	(14)
$\frac{\mathrm{d}[\mathrm{Pr2S6S4}]}{\mathrm{d}t} = \gamma \cdot ([\mathrm{Pr2S6S4}_{\mathrm{T}}] \cdot H(\sigma \cdot W_{\mathrm{s6s4np}}) - [\mathrm{Pr2S6S4}])$ $W_{\mathrm{s6s4np}} = -(\omega_{\mathrm{a,s6s4np3}} \cdot [\mathrm{Cln3}_{\mathrm{N}}] + \omega_{\mathrm{a,s6s4np2}} \cdot [\mathrm{Cln2}] + \omega_{\mathrm{a,s6s4bck2}} \cdot [\mathrm{Bck2}_{\mathrm{T}}] + \omega_{\mathrm{a,s6s4clb5}} \cdot [\mathrm{Clb5}]$ $- \omega_{\mathrm{i,s6s4}}) - \omega_{\mathrm{i,s6s4npclb2}} \cdot [\mathrm{Clb2}]$	(15)[1]
$\frac{\mathrm{d}[\mathrm{Pr2S4P}]}{\mathrm{d}t} = \gamma \cdot ([\mathrm{Pr2S4}_{\mathrm{T}}] \cdot H(\sigma \cdot W_{\mathrm{s4}}) - [\mathrm{Pr2S4P}])$ $W_{\mathrm{s4}} = \omega_{\mathrm{a,s4s4bck2}} \cdot [\mathrm{Bck2}_{\mathrm{T}}] - \omega_{\mathrm{i,s4s4}} - \omega_{\mathrm{i,s4s4clb2}} \cdot [\mathrm{Clb2}]$	(16)
$[\mathrm{Pr2S4}_{\mathrm{T}}] =$ $\min(\max(0, [\mathrm{Pr2}] - [\mathrm{Pr2S6S4W5}_{\mathrm{T}}] - [\mathrm{Pr2S6S4}_{\mathrm{T}}]), [\mathrm{Swi4}_{\mathrm{T}}] - [\mathrm{Pr2S6S4W5}_{\mathrm{T}}] - [\mathrm{Pr2S6S4}_{\mathrm{T}}] - [\mathrm{Pr5S6S4}_{\mathrm{T}}])$	(17)
$\frac{\mathrm{d}[\mathrm{Pr2S6M1P}]}{\mathrm{d}t} = \gamma \cdot ([\mathrm{Pr2S6M1}_{\mathrm{T}}] \cdot H(\sigma \cdot W_{\mathrm{s6m1}}) - [\mathrm{Pr2S6M1P}])$ $W_{\mathrm{s6m1}} = \omega_{\mathrm{a,s6m1n3}} \cdot [\mathrm{Cln3}_{\mathrm{N}}] + \omega_{\mathrm{a,s6m1bck2}} \cdot [\mathrm{Bck2}_{\mathrm{T}}] + \omega_{\mathrm{a,s6m1n2}} \cdot [\mathrm{Cln2}] + \omega_{\mathrm{a,s6m1clb5}} \cdot [\mathrm{Clb5}] - \omega_{\mathrm{i,s6m1}} - \omega_{\mathrm{i,s6m1clb2}} \cdot [\mathrm{Clb2}]$	(18)
$[\mathrm{Pr2S6M1}_{\mathrm{T}}] = \min(\max(0, [\mathrm{Pr2}] - [\mathrm{Pr2S6S4W5}_{\mathrm{T}}] - [\mathrm{Pr2S6S4}_{\mathrm{T}}] - [\mathrm{Pr2S4}_{\mathrm{T}}]), [\mathrm{S6M1}_{\mathrm{T}}] - [\mathrm{Pr5S6M1}_{\mathrm{T}}])$	(19)
$[\mathrm{S6M1}_{\mathrm{T}}] = \min\left([\mathrm{Mbp1}_{\mathrm{T}}], [\mathrm{Mbp1}_{\mathrm{T}}] \frac{[\mathrm{Swi6}_{\mathrm{T}}]}{[\mathrm{Swi4}_{\mathrm{T}}] + [\mathrm{Mbp1}_{\mathrm{T}}]}\right)$	(20)
$\frac{\mathrm{d}[\mathrm{Pr5S6M1P}]}{\mathrm{d}t} = \gamma \cdot ([\mathrm{Pr5S6M1}_{\mathrm{T}}] \cdot H(\sigma \cdot W_{\mathrm{s6m1}}) - [\mathrm{Pr5S6M1P}])$	(21)
$[\mathrm{Pr5S6M1}_{\mathrm{T}}] = \min(0.85 \cdot [\mathrm{Pr5}], [\mathrm{S6M1}_{\mathrm{T}}])$	(22)[2]
$\frac{\mathrm{d}[\mathrm{Pr5S6S4P}]}{\mathrm{d}t} = \gamma \cdot ([\mathrm{Pr5S6S4}_{\mathrm{T}}] \cdot H(\sigma \cdot W_{\mathrm{s6s4}}) - [\mathrm{Pr5S6S4P}])$	(23)
$[\mathrm{Pr5S6S4}_{\mathrm{T}}] = \min(0.15 \cdot [\mathrm{Pr5}], [\mathrm{S6S4}_{\mathrm{T}}] - [\mathrm{Pr2S6S4W5}_{\mathrm{T}}] - [\mathrm{Pr2S6S4}_{\mathrm{T}}])$	(24)[2]
$\frac{\mathrm{d}[\mathrm{BUD}]}{\mathrm{d}t} = k_{\mathrm{s,bud}} \cdot (e_{\mathrm{budn3}} \cdot [\mathrm{Cln3}_{\mathrm{N}}] + e_{\mathrm{budn2}} \cdot [\mathrm{Cln2}] + e_{\mathrm{budclb5}} \cdot [\mathrm{Clb5}]) - k_{\mathrm{d,bud}} \cdot [\mathrm{BUD}]$	(25)[3]
S/G$_2$/M Module	

$\frac{\mathrm{d}[\mathrm{Clb5_T}]}{\mathrm{d}t} = \left(k_{\mathrm{s,clb5}} \cdot \left(1 + 0.2 \cdot \max\left(0, [\mathrm{Pr5}] - [\mathrm{Pr5S6M1_T}] - [\mathrm{Pr5S6S4_T}]\right)\right) + k_{\mathrm{s,clb5,mbf}} \cdot V_{\mathrm{S5}}\right) \cdot (1 - e^{-V/v_{\mathrm{clb5}}})$ $- (k_{\mathrm{d,clb5}} + k_{\mathrm{d,clb5,20}} \cdot [\mathrm{Cdc20_A : APCP}] + k_{\mathrm{d,clb5,20i}} \cdot [\mathrm{Cdc20_A : APC}]) \cdot [\mathrm{Clb5_T}]$ $V_{\mathrm{S5}} = e_{\mathrm{5,s6m}} \cdot [\mathrm{Pr5S6M1P}] + e_{\mathrm{5,s6s4}} \cdot [\mathrm{Pr5S6S4P}]$	(26)
$\frac{\mathrm{d}[\mathrm{Clb2_T}]}{\mathrm{d}t} = (k_{\mathrm{s,clb2}} + k_{\mathrm{s,clb2,m1}} \cdot [\mathrm{Mcm1_A}]) \cdot (1 - e^{-V/v_{\mathrm{clb2}}})$ $- (k_{\mathrm{d,clb2}} + k_{\mathrm{d,clb2,20}} \cdot [\mathrm{Cdc20_A : APCP}] + k_{\mathrm{d,clb2,20i}} \cdot [\mathrm{Cdc20_A : APC}] + k_{\mathrm{d,clb2,h1}} \cdot [\mathrm{Cdh1_A}]) \cdot [\mathrm{Clb2_T}]$	(27)
$\frac{\mathrm{d}[\mathrm{CKI_T}]}{\mathrm{d}t} = k_{\mathrm{s,cki}} + k_{\mathrm{s,cki,swi5}} \cdot [\mathrm{Swi5_A}] - k_{\mathrm{d,cki}} \cdot ([\mathrm{CKI_T}] - [\mathrm{CKIP}]) - k_{\mathrm{d,ckip}} \cdot [\mathrm{CKIP}]$	(28)
$\frac{\mathrm{d}[\mathrm{CKIP}]}{\mathrm{d}t} = \gamma_{\mathrm{cki}} \cdot ([\mathrm{CKI_T}] \cdot H(\sigma \cdot W_{\mathrm{cki}}) - [\mathrm{CKIP}]) - k_{\mathrm{d,ckip}} \cdot [\mathrm{CKIP}]$ $W_{\mathrm{cki}} = \omega_{\mathrm{p,cki,n2}} \cdot [\mathrm{Cln2}] + \omega_{\mathrm{p,cki,b5}} \cdot [\mathrm{Clb5}] + \omega_{\mathrm{p,cki,b2}} \cdot [\mathrm{Clb2}] - \omega_{\mathrm{dp,cki}} - \omega_{\mathrm{dp,cki,14}} \cdot [\mathrm{Cdc14}]$	(29)
$[\mathrm{Clb5}] = \max\left(0, [\mathrm{Clb5_T}] \cdot \left(1 - \frac{h_{\mathrm{sic1}} \cdot [\mathrm{CKI_T}]}{[\mathrm{Clb5_T}] + [\mathrm{Clb2_T}] + \mathrm{CLB2nd}}\right)\right)$ h_{sic1} = 0 only when SIC1 is deleted and h_{sic1} = 1 otherwise CLB2nd=0 and non-zero only when non-degradable Clb2 is present	(30)
$[\mathrm{Clb2_F}] = \max\left(0, ([\mathrm{Clb2_T}] + \mathrm{CLB2nd}) \cdot \left(1 - \frac{h_{\mathrm{CDC6}} \cdot [\mathrm{CKI_T}]}{h_{\mathrm{sic1}} \cdot [\mathrm{Clb5_T}] + [\mathrm{Clb2_T}] + \mathrm{CLB2nd}}\right)\right)$ $h_{\mathrm{CDC6}} > 1$ only when CDC6 is overexpressed and $h_{\mathrm{CDC6}} = 1$ otherwise CLB2nd=0 and non-zero only when non-degradable Clb2 is present	(31)
$[\mathrm{Clb2}] = [\mathrm{Clb2_F}] \cdot (1 - H(\sigma \cdot W_{\mathrm{clb2}}))$ $W_{\mathrm{clb2}} = \omega_{\mathrm{dp,clb2}} - \omega_{\mathrm{p,clb2,we}} \cdot [\mathrm{Swe1_T}]$	(32)
$\frac{\mathrm{d}[\mathrm{Swe1_T}]}{\mathrm{d}t} = k_{\mathrm{s,swe1}} + k_{\mathrm{s,swe1,sbf}} \cdot V_{\mathrm{S2}}$ $- (k_{\mathrm{d,swe1}} + k_{\mathrm{d,swe1,h1}} \cdot [\mathrm{Cdh1_A}]) \cdot ([\mathrm{Swe1_T}] - [\mathrm{Swe1P}]) - (k_{\mathrm{d,swe1p}} + k_{\mathrm{d,swe1p,h1}} \cdot [\mathrm{Cdh1_A}]) \cdot [\mathrm{Swe1P}]$	(33)
$\frac{\mathrm{d}[\mathrm{Swe1P}]}{\mathrm{d}t} = \gamma \cdot ([\mathrm{Swe1_T}] \cdot H(\sigma \cdot W_{\mathrm{swe1}}) - [\mathrm{Swe1P}]) - (k_{\mathrm{d,swe1p}} + k_{\mathrm{d,swe1p,h1}} \cdot [\mathrm{Cdh1_A}]) \cdot [\mathrm{Swe1P}]$ $W_{\mathrm{swe1}} = \omega_{\mathrm{p,swe1,b2}} \cdot [\mathrm{Clb2}] - \omega_{\mathrm{dp,swe1}}$	(34)
$\frac{\mathrm{d}[\mathrm{Swi5_T}]}{\mathrm{d}t} = k_{\mathrm{s,swi5}} + k_{\mathrm{s,swi5,m1}} \cdot [\mathrm{Mcm1_A}] - k_{\mathrm{d,swi5}} \cdot [\mathrm{Swi5_T}]$	(35)

$[\mathrm{Swi5_A}] = [\mathrm{Swi5_T}] \cdot H(\sigma \cdot W_{\mathrm{swi5}})$ $W_{\mathrm{swi5}} = \omega_{\mathrm{a,swi5}} + \omega_{\mathrm{a,swi5,14}} \cdot [\mathrm{Cdc14}] - \omega_{\mathrm{i,swi5,b2}} \cdot [\mathrm{Clb2}]$	(36)
$\frac{\mathrm{d}[\mathrm{ORI}]}{\mathrm{d}t} = k_{\mathrm{s,ori,e}} \cdot (e_{\mathrm{ori,b5}} \cdot [\mathrm{Clb5}] + e_{\mathrm{ori,b2}} \cdot [\mathrm{Clb2}]) - k_{\mathrm{d,ori}} \cdot [\mathrm{ORI}]$	(37)[3]
$\frac{\mathrm{d}[\mathrm{Cdh1_A}]}{\mathrm{d}t} = \gamma \cdot ([\mathrm{Cdh1_T}] \cdot H(\sigma \cdot W_{\mathrm{cdh1}}) - [\mathrm{Cdh1_A}])$ $W_{\mathrm{cdh1}} = \omega_{\mathrm{a,cdh1}} + \omega_{\mathrm{a,cdh1,14}} \cdot [\mathrm{Cdc14}] - (\omega_{\mathrm{i,cdh1,n2}} \cdot [\mathrm{Cln2}] + \omega_{\mathrm{i,cdh1,b5}} \cdot [\mathrm{Clb5}] + \omega_{\mathrm{i,cdh1,b2}} \cdot [\mathrm{Clb2}])$	(38)
$[\mathrm{Mcm1_A}] = [\mathrm{Mcm1_T}] \cdot H(\sigma \cdot W_{\mathrm{mcm1}})$ $W_{\mathrm{mcm1}} = \omega_{\mathrm{a,mcm1,b2}} \cdot [\mathrm{Clb2}] - \omega_{\mathrm{i,mcm1}}$	(39)
$\frac{\mathrm{d}[\mathrm{APCP}]}{\mathrm{d}t} = \gamma_{\mathrm{apc}} \cdot ([\mathrm{APC_T}] \cdot H(\sigma \cdot W_{\mathrm{apc}}) - [\mathrm{APCP}])$ $W_{\mathrm{apc}} = \omega_{\mathrm{a,apc,b2}} \cdot [\mathrm{Clb2}] - \omega_{\mathrm{i,apc}}$	(40)
$\frac{\mathrm{d}[\mathrm{Mad2_A}]}{\mathrm{d}t} = \gamma \cdot ([\mathrm{Mad2_T}] \cdot H(\sigma \cdot W_{\mathrm{mad2}}) - [\mathrm{Mad2_A}])$ $W_{\mathrm{mad2}} = \omega_{\mathrm{a,mad2}} \cdot \mathrm{SAC} - \omega_{\mathrm{i,mad2}}$, SAC = 1 ((HU = 1) or (for ([ORI] ≥ 1) & (ORI was reset to 0 before) and [SPN] < 1)) or 0 (otherwise) HU = 1 in hydroxyurea and HU = 0 otherwise	(41)
$\frac{\mathrm{d}[\mathrm{Cdc20_T}]}{\mathrm{d}t} = k_{\mathrm{s,cdc20}} + k_{\mathrm{s,cdc20,m1}} \cdot [\mathrm{Mcm1_A}] - k_{\mathrm{d,cdc20}} \cdot [\mathrm{Cdc20_T}]$	(42)
$[\mathrm{Cdc20_A}] = \max(0, [\mathrm{Cdc20_T}] - [\mathrm{Mad2_A}])$	(43)
$[\mathrm{Cdc20_A : APCP}] = \min([\mathrm{Cdc20_A}], [\mathrm{APCP}])$	(44)
$[\mathrm{Cdc20_A : APC}] = \min([\mathrm{Cdc20_A}] - [\mathrm{Cdc20_A : APCP}], [\mathrm{APC_T}] - [\mathrm{APCP}])$	(45)
$\frac{\mathrm{d}[\mathrm{SPN}]}{\mathrm{d}t} = k_{\mathrm{s,spn}} \cdot B_{\mathrm{spn}} - k_{\mathrm{d,spn}} \cdot [\mathrm{SPN}]$, $B_{\mathrm{spn}} = 1$ (for $[\mathrm{Clb2}] \geq J_{\mathrm{spn}}$) or 0 (otherwise)	(46)[3]
EXIT Module	
$\frac{\mathrm{d}[\mathrm{Pds1_T}]}{\mathrm{d}t} = k_{\mathrm{s,pds1}} + k_{\mathrm{s,pds1,mbf}} \cdot V_{\mathrm{S5}} - (k_{\mathrm{d,pds1}} + k_{\mathrm{d,pds1,20}} \cdot [\mathrm{Cdc20_A : APCP}] + k_{\mathrm{d,pds1,20i}} \cdot [\mathrm{Cdc20_A : APC}]) \cdot [\mathrm{Pds1_T}]$	(47)

$[\mathrm{Esp1}] = \max(0, [\mathrm{Esp1_T}] - [\mathrm{Pds1_T}])$	(48)
$\frac{\mathrm{d}[\mathrm{Cdc55_A}]}{\mathrm{d}t} = \gamma \cdot ([\mathrm{Cdc55_T}] \cdot H(\sigma \cdot W_{\mathrm{c55}}) - [\mathrm{Cdc55_A}])$ $W_{\mathrm{c55}} = -\omega_{\mathrm{i,cdc55,p1}} \cdot [\mathrm{Esp1}]$	(49)
$\frac{\mathrm{d}[\mathrm{Net1_A}]}{\mathrm{d}t} = \gamma \cdot ([\mathrm{Net1_T}] \cdot H(\sigma \cdot W_{\mathrm{net1}}) - [\mathrm{Net1_A}])$ $W_{\mathrm{net1}} = \omega_{\mathrm{dp,net1}} + \omega_{\mathrm{dp,net1,14}} \cdot [\mathrm{Cdc14n}] + \omega_{\mathrm{dp,net1,c55}} \cdot [\mathrm{Cdc55_A}]$ $- [\mathrm{Cdc5_A}] \cdot (\omega_{\mathrm{p,net1}} + \omega_{\mathrm{p,net1,b2}} \cdot [\mathrm{Clb2}] + \omega_{\mathrm{p,net1,en}} \cdot [\mathrm{Tem1_A} : \mathrm{Cdc15_A}] + \omega_{\mathrm{p,net1,15}} \cdot [\mathrm{Cdc15_{AF}}])$	(50)
$[\mathrm{Cdc15_{AF}}] = \max(0, [\mathrm{Cdc15_A}] - [\mathrm{Tem1_A}])$	(51)
$\frac{\mathrm{d}[\mathrm{Cdc14c}]}{\mathrm{d}t} = r_{\mathrm{cdc14,n\to c}} \cdot [\mathrm{Cdc14n}] \cdot [\mathrm{Tem1_A} : \mathrm{Cdc15_A}] - r_{\mathrm{cdc14,c\to n}} \cdot [\mathrm{Cdc14c}]$	(52)
$[\mathrm{Cdc14}] = \max(0, [\mathrm{Cdc14_T}] - \rho_{\mathrm{14,net1}} \cdot [\mathrm{Net1_A}])$	(53)
$[\mathrm{Cdc14n}] = [\mathrm{Cdc14}] - [\mathrm{Cdc14c}]$	(54)
$\frac{\mathrm{d}[\mathrm{Cdc5_T}]}{\mathrm{d}t} = k_{\mathrm{s,polo}} + k_{\mathrm{s,polo,m1}} \cdot [\mathrm{Mcm1_A}] - (k_{\mathrm{d,polo}} + k_{\mathrm{d,polo,h1}} \cdot [\mathrm{Cdh1_A}]) \cdot [\mathrm{Cdc5_T}]$	(55)
$\frac{\mathrm{d}[\mathrm{Cdc5_A}]}{\mathrm{d}t} = \gamma \cdot ([\mathrm{Cdc5_T}] \cdot H(\sigma \cdot W_{\mathrm{polo}}) - [\mathrm{Cdc5_A}])$ $W_{\mathrm{polo}} = \omega_{\mathrm{a,polo,b2}} \cdot [\mathrm{Clb2}] - \omega_{\mathrm{i,polo}}$	(56)
$\frac{\mathrm{d}[\mathrm{Bub2_A}]}{\mathrm{d}t} = \gamma \cdot ([\mathrm{Bub2_T}] \cdot H(\sigma \cdot W_{\mathrm{bub2}}) - [\mathrm{Bub2_A}])$ $W_{\mathrm{bub2}} = \omega_{\mathrm{a,bub2}} + \omega_{\mathrm{a,bub2,14}} \cdot [\mathrm{Cdc14}] + \omega_{\mathrm{a,bub2,c55}} \cdot [\mathrm{Cdc55_A}] - \omega_{\mathrm{i,bub2,lte,lo}} [\mathrm{Cdc5_A}] \cdot \mathrm{I_{SPOC}} - \omega_{\mathrm{i,bub2,lo}} [\mathrm{Cdc5_A}]$ where boolean variable $\mathrm{I_{SPOC}} = \mathrm{SPO} \cdot (1 - \mathrm{NOC}) \cdot (\mathrm{Heav}(\mathrm{TEV} + [\mathrm{Esp1}] - \theta_{\mathrm{cleave}})$ SPO = 1 NOC = 1 in nocodazole and NOC = 0 otherwise TEV = 1 with TEV and TEV = 0 otherwise	(57)
$\frac{\mathrm{d}[\mathrm{Tem1_A}]}{\mathrm{d}t} = \gamma_{\mathrm{tem1}} \cdot ([\mathrm{Tem1_T}] \cdot H(\sigma \cdot W_{\mathrm{tem1}}) - [\mathrm{Tem1_A}])$ $W_{\mathrm{tem1}} = \omega_{\mathrm{a,tem1}} + \omega_{\mathrm{a,tem1,lo}} \cdot [\mathrm{Cdc5_A}] - \omega_{\mathrm{i,tem1,bub2}} \cdot [\mathrm{Bub2_A}]$	(58)

$\frac{\mathrm{d}[\mathrm{Cdc15_A}]}{\mathrm{d}t} = \gamma \cdot ([\mathrm{Cdc15_T}] \cdot H(\sigma \cdot W_{\mathrm{cdc15}}) - [\mathrm{Cdc15_A}])$ $W_{\mathrm{cdc15}} = \omega_{\mathrm{a,cdc15,14}} \cdot [\mathrm{Cdc14}] - \omega_{\mathrm{i,cdc15}} - \omega_{\mathrm{i,cdc15,b2}} \cdot [\mathrm{Clb2}]$	(59)
$[\mathrm{MEN}] = [\mathrm{Tem1_A} : \mathrm{Cdc15_A}] = \min([\mathrm{Tem1_A}], [\mathrm{Cdc15_A}]) \cdot \max(0, [\mathrm{Cdc5_A}])$	(60)
Definition:	
$H(x) = 1/(1+e^{-x})$	
Rules:	
1) Bud emerges when [BUD] = 1. 2) DNA synthesis starts when [ORI] = 1. 3) Spindle assembly is complete and chromosomes are properly aligned when [SPN] = 1. 4) The cell divides asymmetrically between mother and daughter cells when [Clb2] drops below θ_{cd}. The mother:daughter size ratio at birth is 54:46 in glucose medium and 58:42 in galactose and raffinose media. 5) [BUD] is reset to 0 at cell division. 6) [ORI] is reset to 0 (origins of replication are relicensed) and [SPN] is reset to 0 when [Clb2] + [Clb5] drops below θ_{rl}.	
Notes: 1. Equations (13) and (15) describe, respectively, the rates of change of the phosphorylated and non-phosphorylated fractions of total Swi4:Swi6 bound to the *CLN2* promoter Pr2. The effect of [Clb2] on both variables is negative because Clb2-dependent kinase phosphorylates and inactivates both Pr2S6S4P and Pr2S6S4. 2. In Eqs. (22) and (24), we assume that the *CLB5* promoter Pr5 binds both Swi6:Mbp1 and Swi4:Swi6 to an extent of 85% and 15%, respectively, as determined by deBruin et al. (45); see their Supplemental Figure 4. 3. [BUD], [ORI] and [SPN] are variables that integrate the activities of various cyclin-dependent kinases that drive bud initiation, origins of replication and spindle assembly. In each case, we include a small rate constant ($k_{\mathrm{d,bud}}$, $k_{\mathrm{d,ori}}$, $k_{\mathrm{d,spn}}$) representing the activity of an unspecified phosphatase opposing the kinase.	

Table S3. Basal parameter values for wild-type cells.

Rate constants (min^{-1}) (subscripts: "s" for synthesis, "d" for degradation)							
$k_{s,bck2}$	0.13	$k_{d,bck2}$	0.25				
$k_{s,bud,e}$	1.3	$k_{d,bud}$	0.01				
$k_{s,cdc20}$	0.0008	$k_{s,cdc20,m1}$	0.2	$k_{d,cdc20}$	0.32		
$k_{s,cki}$	0.00115	$k_{s,cki,swi5}$	0.02745	$k_{d,cki}$	0.0153	$k_{d,ckip}$	0.5
$k_{s,clb2}$	0.005	$k_{s,clb2,m1}$	0.19772				
$k_{d,clb2}$	0.0086	$k_{d,clb2,20}$	1.142	$k_{d,clb2,20,i}$	0.15	$k_{d,clb2,h1}$	0.6
$k_{s,clb5}$	0.0008	$k_{s,clb5,mbf}$	0.0156				
$k_{d,clb5}$	0.035	$k_{d,clb5,20}$	0.8	$k_{d,clb5,20,i}$	0.25		
$k_{s,cln2}$	0	$k_{s,cln2,sbf}$	0.1	$k_{d,cln2}$	0.135		
$k_{s,cln3}$	0.1	$k_{d,cln3}$	0.2				
$k_{s,ori,e}$	2	$k_{d,ori}$	0.06				
$k_{s,pds1}$	0.03	$k_{s,pds1,mbf}$	0.03				
$k_{d,pds1}$	0.01	$k_{d,pds1,20}$	2.5	$k_{d,pds1,20,i}$	1.7		
$k_{s,polo}$	0	$k_{s,polo,m1}$	0.22	$k_{d,polo}$	0.3	$k_{d,polo,h1}$	1.5
$k_{s,swi5}$	0.005	$k_{s,swi5,m1}$	0.03	$k_{d,swi5}$	0.08		
$k_{s,spn}$	0.24	$k_{d,spn}$	0.03				
$k_{s,swe1}$	0.001	$k_{s,swe1,sbf}$	0.007				
$k_{d,swe1}$	0.01	$k_{d,swe1,h1}$	0.5	$k_{d,swe1p}$	0.2	$k_{d,swe1p,h1}$	0.7
Other time-scale factors (min^{-1})							
μ	0.0077 (MDT = 90 min in glucose medium)						
γ	1	γ_{cki}	10	γ_{apc}	0.5	γ_{tem1}	0.1
Interaction coefficients (dimensionless) (subscripts: "a" for activation, "i" for inactivation, "p" for phosphorylation, "dp" for dephosphorylation)							
$\omega_{a,apc,b2}$	0.625	$\omega_{i,apc}$	0.7				
$\omega_{a,bub2,14}$	0.05	$\omega_{a,bub2}$	2.71	$\omega_{a,bub2,c55}$	0.8	$\omega_{i,bub2,lo}$	3.85
$\omega_{i,bub2,lte,lo}$	6.7						
$\omega_{a,cdc15,14}$	0.85	$\omega_{i,cdc15}$	0.23	$\omega_{i,cdc15,b2}$	0.0149		
$\omega_{i,cdc55,p1}$	0.981						
$\omega_{a,cdh1,14}$	1.1	$\omega_{a,cdh1}$	0.032				
$\omega_{i,cdh1,n2}$	0.9	$\omega_{i,cdh1,b5}$	9.1	$\omega_{i,cdh1,b2}$	0.162		
$\omega_{p,cki,n2}$	1.15	$\omega_{p,cki,b5}$	9.5	$\omega_{p,cki,b2}$	1.65		
$\omega_{dp,cki}$	0.7	$\omega_{dp,cki,14}$	1.747				
$\omega_{dp,clb2}$	1.5	$\omega_{p,clb2,we}$	1.05				

$\omega_{a,mad2}$	30	$\omega_{i,mad2}$	0.6				
$\omega_{a,mcm1,b2}$	10	$\omega_{i,mcm1}$	1.7				
$\omega_{p,net1,b2}$	0.0225	$\omega_{p,net1,en}$	6.6	$\omega_{p,net1,15}$	0.288	$\omega_{p,net1}$	0.22
$\omega_{dp,net1}$	0.055	$\omega_{dp,net1,14}$	2.51	$\omega_{dp,net1,c55}$	1.0		
$\omega_{a,polo,b2}$	4.8	$\omega_{i,polo}$	0.2				
$\omega_{a,s6s4w5,n3}$	8.43	$\omega_{a,s6s4w5,n2}$	0.01	$\omega_{a,s6s4w5,k2}$	2.1	$\omega_{a,s6s4w5,b5}$	0.01
$\omega_{i,s6s4w5}$	0.8	$\omega_{i,s6s4w5,b2}$	2.87				
$\omega_{a,s6s4,n3}$	3.6	$\omega_{a,s6s4,n2}$	0.28	$\omega_{a,s6s4,k2}$	0.6	$\omega_{a,s6s4,b5}$	4.62
$\omega_{i,s6s4}$	0.5	$\omega_{i,s6s4,b2}$	0.035	$\omega_{i,s6s4np,b2}$	0.4		
$\omega_{a,s4s4,k2}$	8.5	$\omega_{i,s4s4}$	0.5	$\omega_{i,s4s4,b2}$	4.5		
$\omega_{a,s6m1,n3}$	3.3	$\omega_{a,s6m1,n2}$	0.2	$\omega_{a,s6m1,k2}$	0.04	$\omega_{a,s6m1,b5}$	6.2
$\omega_{i,s6m1}$	0.5	$\omega_{i,s6m1,b2}$	0.03				
$\omega_{p,ssa1,b2}$	2.0	$\omega_{dp,ssa1}$	1.0				
$\omega_{p,swe1,b2}$	1.5	$\omega_{dp,swe1}$	0.5				
$\omega_{a,swi5,14}$	5.1	$\omega_{a,swi5}$	0.2	$\omega_{i,swi5,b2}$	1.0		
$\omega_{a,tem1,lo}$	1.1	$\omega_{a,tem1}$	0.5	$\omega_{i,tem1,bub2}$	2.5		
Total concentrations (dimensionless)							
$[APC_T]$	25	$[Bub2_T]$	1	$[Cdc14_T]$	2	$[Cdc15_T]$	1
$[Cdc55_T]$	1	$[Cdh1_T]$	1	$[Esp1_T]$	0.5	$[Mad2_T]$	25
$[Mbp1_T]$	5.5	$[Mcm1_T]$	1	$[Net1_T]$	3.55	$[Pr2]$	2
$[Pr5]$	2	$[Ssa1_T]$	1	$[Swi4_T]$	5.5	$[Swi6_T]$	30
$[Tem1_T]$	2	$[Whi5_T]$	10	$[Ydj1_T]$	2.5		
Other parameters (dimensionless)							
$e_{bud,b5}$	0.38	$e_{bud,n2}$	0.45	$e_{bud,n3}$	0.3	$e_{ori,b2}$	0.35
$e_{ori,b5}$	0.5	J_{spn}	0.14	$e_{5,s6m}$	0.16	e_{s4}	0.213
e_{s6m}	0.63	e_{s4s6}	0.216	$e_{5,s6s4}$	1.1	$r_{cdc14,n\to c}$	13
$r_{cdc14,c\to n}$	0.022	v_{bck2}	3	v_{clb2}	1.8	v_{clb5}	0.2
v_{cln3}	12	v_{ydj1}	2.9	θ_{cd}	0.2	θ_{cleave}	0.05
θ_{rl}	0.199	σ	10	$\rho_{14,net1}$	1	f	0.4586

Table S4. List of mutant strains simulated by our model (inconsistencies are highlighted in red and * indicates predictions).

Wild-type
In glucose
In galactose

Start –mutants
mbp1Δ
ssa1Δ
swi4Δ
swi6Δ
swi6Δ in galactose
whi5Δ
ydj1Δ
WHI5^{OP}
bck2Δ mbp1Δ
bck2Δ swi4Δ
bck2Δ swi6Δ
bck2Δ whi5Δ
cln3Δ mbp1Δ
cln3Δ ssa1Δ
cln3Δ swi4Δ
cln3Δ swi6Δ
cln3Δ whi5Δ
cln3Δ ydj1Δ
mbp1Δ swi4Δ
mbp1Δswi6Δ
mbp1Δ whi5Δ
swi4Δ swi6Δ
swi4Δ whi5Δ
swi6Δ whi5Δ
whi5Δ GAL-BCK2
bck2Δ cln3Δ swi6Δ
bck2Δ cln3Δ whi5Δ
bck2Δ swi6Δ sic1Δ
bck2Δ swi6Δ GAL-CLB5*
bck2Δ swi6Δ whi5Δ
cln1Δ cln2Δ mbp1Δ*
cln1Δ cln2Δ swi4Δ
cln1Δ cln2Δ swi6Δ
cln3Δ mbp1Δ swi6Δ*
cln3Δ mbp1Δ multi-copy *BCK2**
cln3Δ mbp1Δ whi5Δ*
cln3Δ swi4Δ sic1Δ*
cln3Δ swi4Δ multi-copy *BCK2**
cln3Δ swi4Δ GAL- BCK2*
cln3Δ swi4Δ whi5Δ*
mbp1Δ swi4Δ GAL- BCK2
mbp1Δ swi4Δ GAL- CLB5*
mbp1Δ swi4Δ GAL-CLN2
mbp1Δ swi4Δ GAL-CLN3*
mbp1Δ swi4Δ cdh1Δ*
mbp1Δ swi4Δ sic1Δ*
mbp1Δ swi4Δ whi5Δ*
swi4Δ swi6Δ sic1Δ
swi4Δ swi6Δ GAL- BCK2
swi4Δ swi6Δ GAL-CLB5*
swi4Δ swi6Δ GAL-CLN2
swi4Δ swi6Δ GAL-CLN3
swi4Δ swi6Δ whi5Δ*
bck2Δ cln3Δ mbp1Δ whi5Δ*
bck2Δ cln3Δ swi4Δ whi5Δ
bck2Δ cln3Δ swi6Δ GAL-CLN3
cln1Δ cln2Δ cln3Δ whi5Δ
cln3Δ swi4Δ whi5Δ sic1Δ*

Bck2 mutants
bck2Δ
Multi-copy *BCK2*
bck2Δ cln3Δ
bck2Δ cln3Δ cdh1Δ*
bck2Δ cln3Δ sic1Δ
bck2Δ cln3Δ GAL-CLB5*
bck2Δ cln3Δ multi-copy *CLN2*
bck2Δ cln3Δ GAL-CLN3
bck2Δ cln3Δ cdc6Δ sic1Δ*
bck2Δ cln3Δ GAL-CLN2

Cln mutants
cln3Δ
GAL-CLN2
GAL-CLN3
cln1Δ cln2Δ
cln1Δcln2Δ bck2Δ
cln1Δ cln2Δ cdh1Δ
cln1Δ cln2Δ cln3Δ
cln1Δ cln2Δ sic1Δ
cln1Δ cln2Δ GAL-SIC1
cln1Δ cln2Δ cdc6Δ *sic1Δ*
cln1Δ cln2Δ bck2Δ cdh1Δ*
cln1Δ cln2Δ cdh1Δ GAL-CLN2
cln1Δ cln2Δ cdh1Δ GAL-SIC1
cln1Δ cln2Δ cln3Δ apc^{ts}
cln1Δ cln2Δ cln3Δ cdh1Δ
cln1Δ cln2Δ cln3Δ sic1Δ
cln1Δ cln2Δ cln3Δ multi-copy *BCK2*
cln1Δ cln2Δ cln3Δ GAL-CLB2
cln1Δ cln2Δ cln3Δ GAL-CLB5
cln1Δ cln2Δ cln3Δ multi-copy *CLB5*
cln1Δ cln2Δ cln3Δ GAL-CLN2
cln1Δ cln2Δ cln3Δ GAL-CLN3
cln1Δ cln2Δ GAL-SIC1 GAL-CLN2
cln1Δ cln2Δ cln3Δ sic1Δ cdc6Δ*
cln1Δ cln2Δ GAL-SIC1 GAL-CLN2 cdh1Δ
cln1Δ cln2Δ cln3Δ bck2Δ GAL-CLN2

Cdh1, Sic1 mutants
cdh1Δ
cdc6Δ
sic1Δ
swi5Δ
GAL-CDC6
Multi-copy *CDC6*
CDH1 constitutively active
SIC1-4A
GAL-SIC1
Multi-copy *SIC1*
Multi-copy *SIC1-high*
GAL-SIC1-dbΔ
GAL-SIC1-4A
cdc6Δ sic1Δ
sic1Δ cdh1Δ
swi5Δ cdh1Δ
sic1Δ GAL-CLB2
cdh1Δ GAL-CLB2
swi5Δ GAL-CLB2
cdh1Δ GAL-CLB5
sic1Δ GAL-CLB5
sic1Δ CLB5-dbΔ
cdc6Δ sic1Δ cdh1Δ
sic1Δ cdh1Δ GAL-CDC20
swi5Δ cdh1Δ GAL-SIC1
SIC1-4A clb5Δ clb6Δ
sic1Δ cdc6Δ cdh1Δ GAL-CDC20

Clb5 Clb6 mutants
clb5Δ
GAL-CLB5
Multi-copy *CLB5*
CLB5-dbΔ
GAL-CLB5-dbΔ
clb5Δ clb6Δ
clb5Δ pds1Δ
CLB5-dbΔ pds1Δ
clb5Δ clb6Δ pds1Δ
clb5Δ pds1Δ + multi-copy *SIC1-high*
clb5Δ clb6Δ cln1Δ cln2Δ
clb5Δ clb6Δ pds1Δ + multi-copy *SIC1-high*

Clb1 Clb2 mutants
GAL-CLB2
CLB2-dbΔ
CLB2-dbΔ in galactose
Multi-copy *GAL-CLB2*
clb1Δ clb2Δ
clb2Δ CLB1
CLB2-dbΔ clb5Δ
CLB2-dbΔ clb5Δ in gal
CLB2-dbΔ GAL-SIC1
CLB2-dbΔ multi-copy *SIC1*
clb2Δ CLB1 cdh1Δ
clb1Δ clb2Δ clb5Δ
clb2Δ CLB1 pds1Δ
CLB2-dbΔ clb5Δ clb6Δ
CLB2-dbΔ clb5Δ clb6Δ in gal
clb1Δ clb2Δ clb5Δ clb6Δ

Cdc20 mutants
cdc20^{ts}
GAL-CDC20
cdc20Δ clb5Δ
cdc20Δ pds1Δ
cdc20Δ GAL-SIC1-4A
cdc20Δ clb5Δ pds1Δ
cdc20Δ pds1Δ cdh1Δ
cdc20Δ pds1Δ CLB5-dbΔ
cdc20Δ pds1Δ SIC1-4A*
cdc20Δ pds1Δ+ multi-copy *SIC1-high*
cdc20Δ clb5Δ clb6Δ pds1Δ
cdc20Δ pds1Δ clb5Δcdh1Δ
cdc20Δ pds1Δ cdh1Δ+ multi-copy *SIC1-high*
cdc20Δ pds1Δ clb5Δ + multi-copy *SIC1-high*
cdc20Δ pds1Δ clb5Δ cdh1Δ + multi-copy *SIC1-high*

APC mutants
APC-A
APC-A cdh1Δ
APC-A cdh1Δ in galactose
APC-A sic1Δ
APC-A GAL-CLB2
APC-A cdc6Δ sic1Δ
APC-A cdh1Δ GAL-CDC6
APC-A cdh1Δ multi-copy *CDC6*
APC-A cdh1Δ GAL-SIC1
APC-A cdh1Δ multi-copy *SIC1*
APC-A chd1Δ multi-copy *CDC20*

Pds1/Esp1 interaction
cdc55Δ
cdc55Δ in galactose
esp1^{ts}
pds1Δ
pds1Δ in galactose
GAL-CDC55
PDS1-dbΔ
GAL-PDS1-dbΔ
GAL-ESP1 cdc20^{ts}
GAL-PDS1-dbΔ esp1^{ts}
GAL-ESP1 GAL-PDS1-dbΔ
cdc20Δ GAL-PDS1-dbΔ GAL-TEV CDC20-back
GAL-TEV cdc20Δ
GAL-ESP1cdc20Δ clb5Δ
GAL-PDS1-dbΔ GAL-TEV cdc20-back
GAL-TEV cdc20Δ clb5Δ
GAL-TEV cdc20Δ GAL- SIC1

Checkpoint mutants
WT in hydroxyurea
WT in nocodazole
bub2Δ
bub2Δ in nocodazole
bub2Δ in hydroxyurea-arrested cells
mad2Δ
mad2Δ in nocodazole
net1^{ts} in nocodazole
pds1Δ in nocodazole
bub2Δ cdc20^{ts}
bub2Δ pds1Δ in nocodazole
mad2Δ bub2Δ
mad2Δ bub2Δ in nocodazole
mad2Δ cdc20^{ts}
mad2Δ pds1Δ in nocodazole
mad2Δ GAL-TEM1 in nocodazole

MEN pathway mutants
cdc15Δ
cdc15^{as1}
lte1Δ
tem1Δ
GAL-CDC15 in hydroxyurea-arrested cells *GAL-CDC15*
Multi-copy *CDC15*
GAL-TEM1
multi-copy *TEM1*
cdc15Δ net1^{ts}
cdc15Δ cdc20-back
lte1Δ bub2Δ
lte1Δ esp1^{ts}
tem1Δ net1^{ts}
cdc15^{ts} multi-copy *CDC14*
cdc15Δ GAL-SIC1
cdc15^{ts} multi-copy *TEM1*
cdc15Δ multi-copy *SWI5*
tem1^{ts} *GAL-CDC15*
tem1Δ multi-copy *CDC14*
tem1^{ts} multi-copy *CDC15*
cdc15Δ net1^{ts} *cdh1Δ*
cdc15^{as1} *cdc20Δ pds1Δ*
cdc15^{as1} *cdc20Δ pds1Δ clb5Δ*
cdc15^{as1} *cdc20Δ pds1Δ clb5Δ clb6Δ*

Exit-from-mitosis mutants
cdc5Δ
cdc14^{ts}
cdc14^{ts} *in galactose*
net1^{ts}
swe1Δ
CDC5-dbΔ
GAL-CDC5
Nocodazole then *GAL-CDC5*
Hydroxyurea then *GAL-CDC5*
GAL-CDC14
GAL-NET1
TAB6-1
cdc5Δ bub2Δ
cdc5Δ cdc15Δ
cdc5Δ net1Δ
cdc5Δ tem1Δ
cdc14^{ts} *cdh1Δ* non-permissive temperature
cdc14^{ts} *sic1Δ* non- permissive temperature
net1^{ts} *cdc20*^{ts}
cdc5Δ GAL-CDC15
cdc5Δ GAL-SIC1
cdc5Δ multi-copy *SWI5*
cdc14-1 GAL-CDC15
bub2Δ GAL-CDC5 in hydroxyurea
GAL-CDC5 cdc15Δ
cdc14^{ts} *GAL-CLN2* non-permissive temp.
cdc14^{ts} *GAL-SIC1*
TAB6-1 cdc15^{ts}
TAB6-1 clb5Δ
GAL-CDC5 cdc20Δ
GAL-CDC14 GAL-NET1
TAB6-1 clb5Δ clb6Δ
TAB6-1 clb2Δ CLB1
GAL-CDC5 GAL-PDS1 cdc20Δ*
cdc20Δ then *GAL-PDS1dbΔ GAL-CDC5*
cdc20Δpds1Δ cdh1Δ then *URL-cdc5*

***Cdc14- oscillating* mutants**
GAL-CLB2-dbΔ
GAL-CLB2nd
GAL-CLB2-dbΔ cdc5-1
GAL-CLB2-dbΔ CDC5-dbΔ
GAL-CLB2-dbΔ cdc14-1
GAL-CLB2-dbΔ cdc15^{as1}
GAL-CLB2-dbΔ cdc20-3
GAL-CLB2-dbΔ cdh1Δ
GAL-CLB2-dbΔ sic1Δ
GAL-CLB2-dbΔ swi5Δ
GAL-CLB2-dbΔ cdc6Δ *sic1Δ**
GAL-CLB2-dbΔ cdc20Δ clb5Δ pds1Δ*
GAL-CLB2nd *cdc5-1*
GAL-CLB2nd *CDC5-dbΔ*
GAL-CLB2nd *cdc14-1*
GAL-CLB2nd *cdc15*^{as1}
GAL-CLB2nd *cdc20-3*
GAL-CLB2nd *cdh1Δ*
GAL-CLB2nd *sic1Δ*
GAL-CLB2nd *swi5Δ*
GAL-CLB2ndcdc6Δ *sic1Δ**
GAL-CLB2nd*cdc20Δ clb5Δ pds1Δ**

Mutant lacking transcription regulation
mbp1Δ mcm1Δ swi4Δ swi5Δ swi6Δ GAL-CLB2 GAL-CDC5 GAL-CDC20 GAL-CLN2(low) GAL-SIC1(low)*

Table S5. Parameter values used to simulate mutant alleles.

Single mutation (deletion)	Modified parameters	Single mutation (overproduction)	Modified parameters
WT in galactose	MDT=150, *f*=0.41556	*APC-A*	$\omega_{a,apc,b2}=0$
WT in hydroxyurea	HU=1, $k_{s,ori,e}=0$, $k_{s,polo,m1}=k_{s,polo,m1}/3$, $k_{s,clb2}=k_{s,clb2}/3$, $k_{s,clb2,m1}=k_{s,clb2,m1}/3$	multi-copy *BCK2*	$k_{s,bck2}=65\cdot k_{s,bck2}$
WT in nocodazole	NOC=1, $k_{s,spn}=0$	*CDC5-db*Δ	$k_{d,polo,h1}=0$
apc^{ts}	$k_{s,cdc20}=0$, $k_{s,cdc20,m1}=0$, $[Cdh1_T]=0$, $[Cdc20_T]=0$	*GAL-CDC5*	$k_{s,polo}=1.2\cdot k_{s,polo,m1}$, MDT=150, *f*=0.41556
*bck2*Δ	$k_{s,bck2}=0$, $[Bck2_T]=0$	*GAL-CDC6*	$h_{CDC6}=3$, MDT=150, f=0.41556
*bub2*Δ	$[Bub2_T]=0$, $[Bub2_A]=0$	multi-copy *CDC6*	$h_{CDC6}=5$
*cdc5*Δ	$k_{s,polo,m1}=0$	*GAL-CDC14*	$[Cdc14_T]=7[Cdc14_T]$, MDT=150, *f*=0.41556
*cdc6*Δ	$k_{s,cki}=k_{s,cki}/3$, $k_{s,cki,swi5}=k_{s,cki,swi5}/3$	multi-copy *CDC14*	$[Cdc14_T]=2[Cdc14_T]$
cdc14^{ts}	$[Cdc14_T]=0$	*GAL-CDC15*	$[Cdc15_T]=10[Cdc15_T]$, MDT=150, *f*=0.41556
cdc14-1	$[Cdc14_T]=0.05$	*multi-copy CDC15*	$[Cdc15_T]=20[Cdc15_T]$
*cdc15*Δ	$[Cdc15_T]=0$	*GAL-CDC55*	$[Cdc55_T]=3[Cdc55_T]$, MDT=150, *f*=0.41556
cdc15^{as1}	$[Cdc15_T]=0.05$	*GAL-CDC20*	$k_{s,cdc20}=3\cdot k_{s,cdc20,m1}$, MDT=150, *f*=0.41556
cdc20^{ts} or *cdc20*Δ	$k_{s,cdc20}=0$, $k_{s,cdc20,m1}=0$, $[Cdc20_T]=0$	*GALL-CDC20*	$k_{s,cdc20}=k_{s,cdc20,m1}$, MDT=150, *f*=0.41556
cdc20-3	$k_{s,cdc20}=0.2\cdot k_{s,cdc20}$, $k_{s,cdc20,m1}=0.2\cdot k_{s,cdc20,m1}$	*CDH1* constitutively active	$\omega_{i,cdh1,b2}=0$, $\omega_{i,cdh1,b5}=0$, $\omega_{i,cdh1,n2}=0$, MDT=150, f=0.41556
*cdc55*Δ	$[Cdc55_T]=0$	*GAL-CLB2*	$k_{s,clb2}=0.2\cdot k_{s,clb2,m1}$, MDT=150, *f*=0.41556
*cdh1*Δ	$[Cdh1_T]=0$, $[Cdh1_A]=0$	*CLB2-db*Δ	$k_{d,clb2,h1}=0.37\cdot k_{d,clb2,h1}$, $k_{d,clb2,20}=0$, $k_{d,clb2,20,i}=0$
*clb5*Δ	$k_{s,clb5}=k_{s,clb5}/10$, $k_{s,clb5,mbf}=k_{s,clb5,mbf}/10$	multi-copy *CLB2* in GAL	$k_{s,clb2}=5\cdot k_{s,clb2}$, $k_{s,clb2,m1}=5\cdot k_{s,clb2,m1}$, MDT=150, *f*=0.41556
*cln3*Δ	$k_{s,cln3}=0$, $[Cln3_T]=0$	*GAL-CLB2-db*Δ (high)	$k_{s,clb2}=1.7\cdot k_{s,clb2,m1}$, $k_{d,clb2,h1}=0.37\cdot k_{d,clb2,h1}$, $k_{d,clb2,20}=0$, $k_{d,clb2,20,i}=0$, MDT=150, *f*=0.41556
esp1^{ts}	$[Esp1_T]=0.081$	*GAL-CLB2*nd	CLB2nd=3, MDT=150, *f*=0.41556
*lte1*Δ	$\omega_{i,bub2,lte,lo}=0$	*GAL-CLB5*	$k_{s,clb5}=2.2\cdot k_{s,clb5,mbf}$, MDT=150, *f*=0.41556
*mad2*Δ	$\omega_{a,mad2}=0$, $[Mad2_A]=0$	multi-copy *CLB5*	$k_{s,clb5}=5\cdot k_{s,clb5}$, $k_{s,clb5,mbf}=5\cdot k_{s,clb5,mbf}$
*mbp1*Δ	$[Mbp1_T]=0$	*CLB5-db*Δ	$k_{d,clb5,20}=0$, $k_{d,clb5,20,i}=0$
net1^{ts}	$\rho_{14,net1}=0.25$	*GAL-CLN2*	$k_{s,cln2}=0.06$, MDT=150, *f*=0.41556

*pds1*Δ	$k_{s,pds1}$=0, $k_{s,pds1,mbf}$ =0	*GAL-CLN2(low)*	$k_{s,cln2}$=0.01, MDT=150, *f*=0.41556
*sic1*Δ	$k_{s,cki} = k_{s,cki}$ 2/3, $k_{s,cki,swi5} = k_{s,cki,swi5}$ 2/3, h_{sic1}=0, [CKI_T]=2[CKI_T]/3	multi-copy *CLN2*	$k_{s,cln2,sbf} = 5 \cdot k_{s,cln2,sbf}$
*ssa1*Δ	[$Ssa1_T$]=0	*GAL-CLN3*	$k_{s,cln3} = 7 \cdot k_{s,cln3}$, MDT=150, *f*=0.41556
*swe1*Δ	$k_{s,swe1}$=0, $k_{s,swe1,sbf}$ =0	*GAL-ESP1*	[$Esp1_T$]= 5.8[$Esp1_T$], MDT=150, *f*=0.41556
*swi4*Δ	[$Swi4_T$]=0	*GAL-NET1*	[$Net1_T$]= 4[$Net1_T$], $\omega_{dp,net1,14} = \omega_{dp,net1,14}/4, \omega_{dp,net1,c55} = \omega_{dp,net1,c55}/4,$ $\omega_{p,net1} = \omega_{p,net1}/4, \omega_{p,net1,b2} = \omega_{p,net1,b2}/4$ $\omega_{p,net1,en} = \omega_{p,net1,en}/4, \omega_{p,net1,15} = \omega_{p,net1,15}/4$ MDT=150, *f*=0.41556
*swi5*Δ	$k_{s,swi5}$=0, $k_{s,swi5,m1}$=0	*PDS1-db*Δ	$k_{d,pds1,20}$=0, $k_{d,pds1,20,i}$=0
*swi6*Δ	[$Swi6_T$]=0	*GAL-PDS1-db*Δ	$k_{s,pds1} = 5 \cdot k_{s,pds1}, k_{d,pds1,20}$=0, $k_{d,pds1,20,i}$=0, MDT=150, *f*=0.41556
*tem1*Δ	[$Tem1_T$]=0	*SIC1-4A*	$\omega_{p,cki,b2}$=0, $\omega_{p,cki,b5}$=0, $\omega_{p,cki,n2}$=0
*whi5*Δ	[$Whi5_T$]=0	*GAL-SIC1*	MDT=150, *f*=0.41556, $k_{s,cki} = 0.55 \cdot k_{s,cki,swi5}$
*ydj1*Δ	k_{ydj1}=0	*GAL-SIC1(low)*	MDT=150, *f*=0.41556, $k_{s,cki} = 0.21 \cdot k_{s,cki,swi5}$
*cdc6*Δ *sic1*Δ	$k_{s,cki}$=0, $k_{s,cki,swi5}$=0	multi-copy *SIC1*	$k_{s,cki} = 3 \cdot k_{s,cki}$, $k_{s,cki,swi5} = 3 \cdot k_{s,cki,swi5}$
*clb1*Δ *clb2*Δ	$k_{s,clb2}$ =0, $k_{s,clb2,m1}$=0	multi-copy *SIC1-high*	$k_{s,cki} = 36 \cdot k_{s,cki}$, $k_{s,cki,swi5} = 36 \cdot k_{s,cki,swi5}$
*clb2*Δ *CLB1*	$k_{s,clb2} = k_{s,clb2}/2$, $k_{s,clb2,m1} = k_{s,clb2,m1}/2$	*GAL-SIC1-db*Δ	$k_{s,cki}$=0.55 $\cdot k_{s,cki,swi5}$, $k_{d,ckip}$=0, MDT=150, *f*=0.41556
*clb5*Δ *clb6*Δ	$k_{s,clb5}$=0, $k_{s,clb5,mbf}$ =0	*GAL-SIC1-4A*	$\omega_{p,cki,b2}$=0, $\omega_{p,cki,b5}$=0, $\omega_{p,cki,n2}$=0, $k_{s,cki}$= $15 \cdot k_{s,cki,swi5}$, MDT=150, *f*=0.41556
*cln1*Δ *cln2*Δ	$k_{s,cln2,sbf}$ =0, [Cln2]=0	*TAB6-1*	$\rho_{14,net1}$=0.3
		GAL-TEM1	[$Tem1_T$]=10[$Tem1_T$], MDT=150, f=0.41556
		multi-copy *TEM1*	[$Tem1_T$]=10[$Tem1_T$]
		GAL-TEV	TEV=1, MDT=150, *f*=0.41556
		WHI5^{OP}	$\omega_{p,s6s4pwn3} = \omega_{p,s6s4pwn3}/2, \omega_{p,s6s4pwn2} = \omega_{p,s6s4pwn2}/2,$ $\omega_{p,s6s4pwk2} = \omega_{p,s6s4pwk2}/2, \omega_{p,s6s4pwb5} = \omega_{p,s6s4pwb5}/2$

Table S6. START mutant strains discussed in the main text of the manuscript.

Mutant Genotype	Observed Phenotype (simulation result)	References
ssa1Δ	viable (cell size: 0.8x)	(29)
ydj1Δ	viable (cell size: 1.85x)	(30)
swi4Δ	viable (cell size: 1.9x)	(6)
swi6Δ	viable (cell size: 2.4x)	(6)
mbp1Δ	viable (cell size: 1.0x)	(46)
swi4Δ swi6Δ	inviable (G1 arrest)	(46)
swi4Δ mbp1Δ	inviable (G1 arrest)	(46)
whi5Δ	viable (cell size: 0.63x)	(30)
$WHI5^{0P}$	viable (cell size: 1.49x)	(5)
cln3Δ	viable (cell size: 1.85x)	(5)
cln3Δ whi5Δ	viable (cell size: 0.63x)	(4, 5)
cln3Δ mbp1Δ	viable (cell size 1.84x)	(40)
cln3Δ swi6Δ	viable (cell size: 2.4x)	(6)
cln3Δ swi4Δ	inviable (G1 arrest)	(47)
cln3Δ bck2Δ	G1 arrest (G1 arrest)	(48)
cln3Δ bck2Δ whi5Δ	viable (cell size: 1.48x)	(4, 5)
cln1Δ cln2Δ cln3Δ	inviable (G1 arrest)	(49)
cln1Δ cln2Δ cln3Δ sic1Δ	viable (cell size: 1.44x)	(50, 51)
cln1Δ cln2Δ cln3Δ GAL-CLB5	viable (cell size: 0.43xWT in GAL)	(41, 52)
cln3Δ bck2Δ sic1Δ	inviable (G1 arrest)	(48)
cln1Δ cln2Δ cln3Δ cdh1Δ	telophase arrest (T arrest)	(53)
cln1Δ cln2Δ cdh1Δ	viable (cell size: 1x)	(22)
cln1Δ cln2Δ	viable (cell size: 2.3x)	(54)
swi4Δ swi6Δ sic1Δ	inviable (G1 arrest)	(48)
bck2Δ swi6Δ sic1Δ	inviable (G1 arrest)	(55)
cln1Δ cln2Δ swi4Δ	inviable (G1 arrest)	(56)
cln1Δ cln2Δ cln3Δ whi5Δ	inviable (G1 arrest)	(4)
swi4Δ mbp1Δ GAL-BCK2	inviable (G1 arrest)	(48)

Table S7. FINISH mutant strains discussed in the main text of the manuscript.

Mutant Genotype	Observed Phenotype (simulation result)	Ref.
cdc14Δ	telophase arrest (T arrest)	(57)
pds1Δ	viable (cell size: 0.98x)	(58)
cdc55Δ	viable (cell size: 0.997x)	(59)
cdc20Δ	metaphase arrest (M arrest)	(60)
cdc20Δ pds1Δ	telophase arrest (T arrest)	(25)
cdc20Δ pds1Δ clb5Δ	viable (cell size: 1.0x)	(25)
cdc20Δ pds1Δ clb5Δ cdh1Δ	telophase arrest (T arrest)	(25, 61)
cdc20Δ pds1Δ cdh1Δ + multi-copy SIC1	inviable (dies after 7 cycles)	(25, 61)
cdc20Δ pds1Δ clb5Δ cdh1Δ + multi-copy SIC1	viable (cell size: 0.75x)	(25, 61)
cdc15Δ	telophase arrest (T arrest, Cdc14 is released and then comes back)	(62)
esp1Δ	inviable (mitotic exit is delayed 7.8 min)	(63)
cdc20Δ PDS1-dbΔ CDC20-back	inviable (M arrest)	(63, 64)
cdc20Δ GAL-PDS1-dbΔ GAL-TEV CDC20-back	mitotic exit delayed (mitotic exit with 3 min delay)	(65)
bub2Δ	viable (cell size: 1.0x)	(66)
tem1Δ	telophase arrest (T arrest)	(67)
tem1^{ts} multi-copy CDC15	viable (cell size: 1.0x)	(38)
cdc15^{ts} multi-copy TEM1	telophase arrest (T arrest)	(38)
cdc15^{ts} net1^{ts}	viable (cell size: 1.26x)	(68)
tem1^{ts} net1^{ts}	viable (cell size: 1.25x)	(69)
cdc15^{ts} multi-copy CDC14	viable (cell size: 1.06x)	(38)
cdc5Δ	inviable, no Cdc14 release (T arrest)	(64, 70)
net1^{ts} cdc15Δ cdh1Δ	viable (cell size: 0.99x)	(69)
GAL-CDC5	viable (cell size: 1.1xWT in GAL)	(71)
cdc20Δ GAL-PDS1-dbΔ GAL-CDC5	inviable, Cdc14 is released (arrested, then Cdc14 released)	(72)
HU then GAL-CDC5	inviable, Cdc14 is released (arrested, then Cdc14 released)	(73, 74)
NOC then GAL-CDC5	inviable, Cdc14 is released (arrested, then	(72)

	Cdc14 released)	
GAL-CLB2-dbΔ	Cdc14 oscillations (Cdc14 oscillations)	(31)
GAL-CLB2nd	Cdc14 oscillations (Cdc14 oscillations)	(33)
GAL-CLB2-dbΔ cdc15^{as1}	Cdc14 oscillations (Cdc14 oscillations)	(31)
GAL-CLB2-dbΔ sic1Δ	Cdc14 oscillations (Cdc14 oscillations)	(31)
GAL-CLB2-dbΔ swi5Δ	Cdc14 oscillations (Cdc14 oscillations)	(31)
GAL-CLB2-dbΔ cdc20-3	Cdc14 oscillations (Cdc14 oscillations)	(31)
GAL-CLB2-dbΔ cdc5-1	telophase arrest, no Cdc14 oscillations (T arrest, no Cdc14 oscillations, Cdc14 is not released)	(31)
GAL-CLB2-dbΔ GAL-CDC5-dbΔ	telophase arrest, no Cdc14 oscillations (T arrest, no Cdc14 oscillations, Cdc14 is released)	(31)
GAL-CLB2-dbΔ cdh1Δ	telophase arrest, no Cdc14 oscillations (T arrest, no Cdc14 oscillations, Cdc14 is released)	(31)
GAL-CLB2-dbΔ cdc14-1	telophase arrest, no Cdc14 oscillations (T arrest, no Cdc14 oscillations)	(31)
lte1Δ	viable, cold sensitive (cell size: 1.02x)	(37)
cdc14Δ GAL-SIC1	partially viable (viable, cell size: 1.03xWT in GAL)	(38)
CLB2-dbΔ clb5Δ in galactose	viable (viable, cell size: 1.25xWT in GAL)	(39)

Table S8. Predicted phenotypes of novel mutant strains according to the basal parameter set.

Mutant Genotype	Predicted Phenotype	Mutant Genotype	Predicted Phenotype
cln1Δ cln2Δ mbp1Δ	viable, cell size: 3.49x	*bck2Δ cln3Δ GAL-CLB5*	viable, cell size: 0.43xWT in GAL
cln1Δ cln2Δ cln3Δ cdc6Δ sic1Δ	viable, cell size: 1.4x	*bck2Δ swi6Δ GAL-CLB5*	viable, cell size: 0.43xWT in GAL
cln3Δ swi4Δ whi5Δ	inviable, G1 arrest	*cln3Δ swi4Δ whi5Δ sic1Δ*	inviable, the third division has mass >10x WT and mass continues to grow
swi4Δ mbp1Δ whi5Δ	inviable, G1 arrest	*bck2Δ cln3Δ whi5Δ mbp1Δ*	viable, cell size: 1.3x
swi4Δ mbp1Δ sic1Δ	inviable, G1 arrest	*swi4Δ swi6Δ whi5Δ*	inviable, G1 arrest
swi4Δ mbp1Δ cdh1Δ	inviable, G1 arrest	*swi4Δ swi6Δ GAL-CLB5*	viable, cell size: 0.43xWT in GAL
swi4Δ mbp1Δ GAL-CLN3	inviable, G1 arrest	*cln1Δ cln2Δ bck2Δ cdh1Δ*	viable, cell size: 1.17x
swi4Δ mbp1Δ GAL-CLB5	viable, cell size: 0.43x WT in GAL	*cln3Δ bck2Δ cdh1Δ*	inviable, T arrest
mbp1Δ mcm1Δ swi4Δ swi5Δ swi6Δ GAL-CLB2 GAL-CDC5 GAL-CDC20 GAL-CLN2(low) GAL-SIC1(low)	viable, cell size: 0.95x WT in GAL	*bck2Δ cln3Δ cdc6Δsic1Δ*	inviable, the third division has mass >10x WT and mass continues to grow
cln3Δ mbp1Δ swi6Δ	viable, cell size: 2.4x	*GAL-CLB2-dbΔ* cdc6Δ *sic1Δ*	arrests in telophase, Cdc14 oscillations
cln3Δ mbp1Δ whi5Δ	viable, cell size: 0.63x	*GAL-CLB2-dbΔ pds1Δ cdc20Δ clb5Δ*	arrests in telophase, Cdc14 oscillations
cln3Δ mbp1Δ multi-copy BCK2	viable, cell size: 0.63x	*GAL-CLB2nd*cdc6Δ *sic1Δ*	arrests in telophase, Cdc14 oscillations
cln3Δ swi4Δ multi-copy BCK2	viable, cell size: 0.65x	*GAL-CLB2ndcdc20Δ clb5Δ pds1Δ*	arrests in telophase, Cdc14 oscillations
cln3Δ swi4Δ GAL- BCK2	viable, cell size: 0.76x WT in GAL	*GAL-CDC5GAL-PDS1-dbΔ cdc20Δ*	inviable, Cdc14 is released
cln3Δ swi4Δ sic1Δ	inviable, the third division has mass >10x WT and mass continues to grow	*cdc20Δ pds1Δ SIC1-4A*	inviable, M arrest

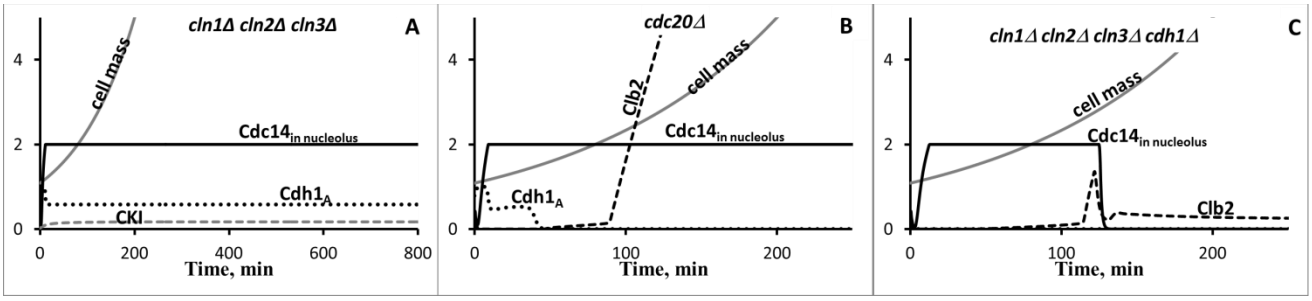

Figure S1. The example of inviable phenotypes: *cln1Δ cln2Δ cln3Δ* is arrested in G1 phase, Clb2 and Clb5 are inhibited due to high level of Cdh1 and CKI in this mutant which results in origin activation failure (panel A); *cdc20Δ* strain is arrested in M phase, Clb2 goes to high and Cdc14 is not released from the nucleolus (panel B); *cln1Δ cln2Δ cln3Δ cdh1Δ* strain is arrested in Telophase, despite Cdc14 release from nucleolus Clb2 never drops below θ_{cd} threshold to trigger the cell division (panel C).

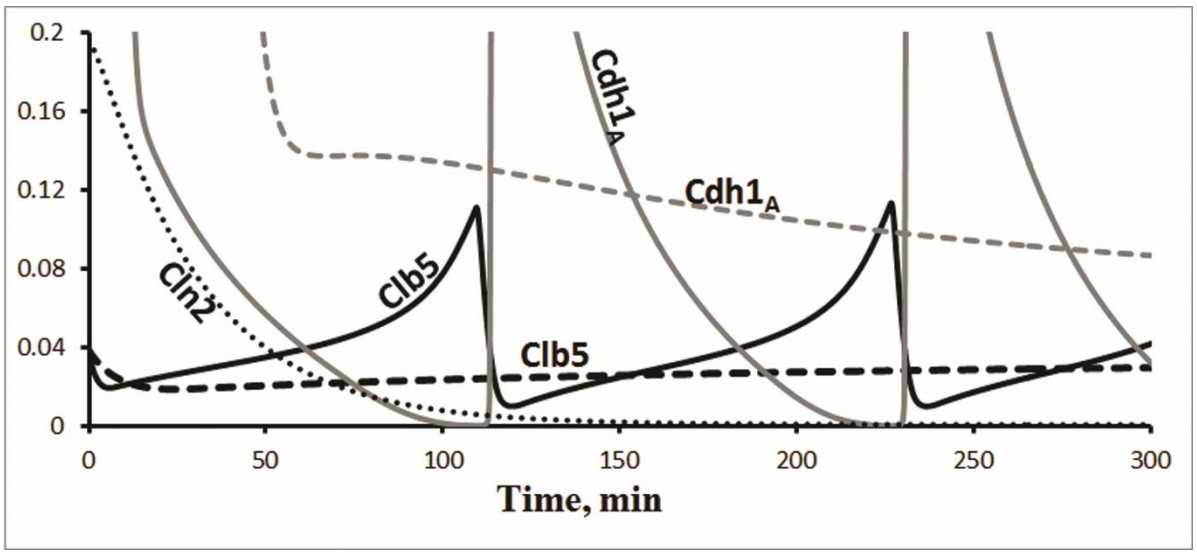

Figure S2. Cyclin and APC:Cdh1 concentrations in *cln3Δ bck2Δ sic1Δ* cells (dashed lines) and *cln1Δ cln2Δ cln3Δ sic1Δ* cells (solid lines). In the *cln3Δ bck2Δ sic1Δ* strain, neither SBF nor MBF is active, thus Clb5 level is low and Cdh1:APC is active. By comparison, in the *cln1Δ cln2Δ cln3Δ sic1Δ* strain, the amount of Clb5 is higher and hence the activity of Cdh1:APC is lower. This explains why the former strain is inviable and the latter is viable.

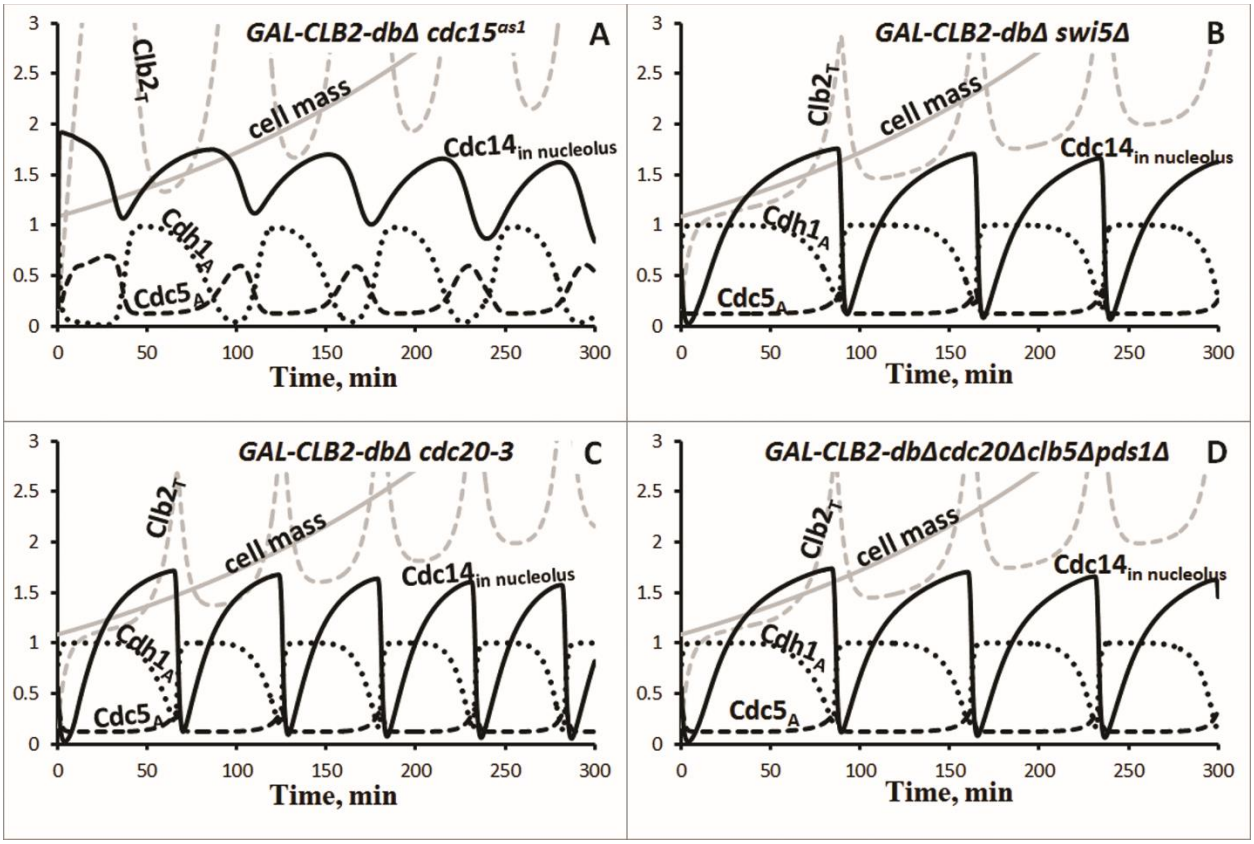

Figure S3. Cdc14 endocycles are independent of the MEN pathway (A), of the Swi5 transcription factor (B), of the Sic1 inhibitor (C), and of the FEAR pathway (D). Compare to (31). Panel D is a prediction of the model.

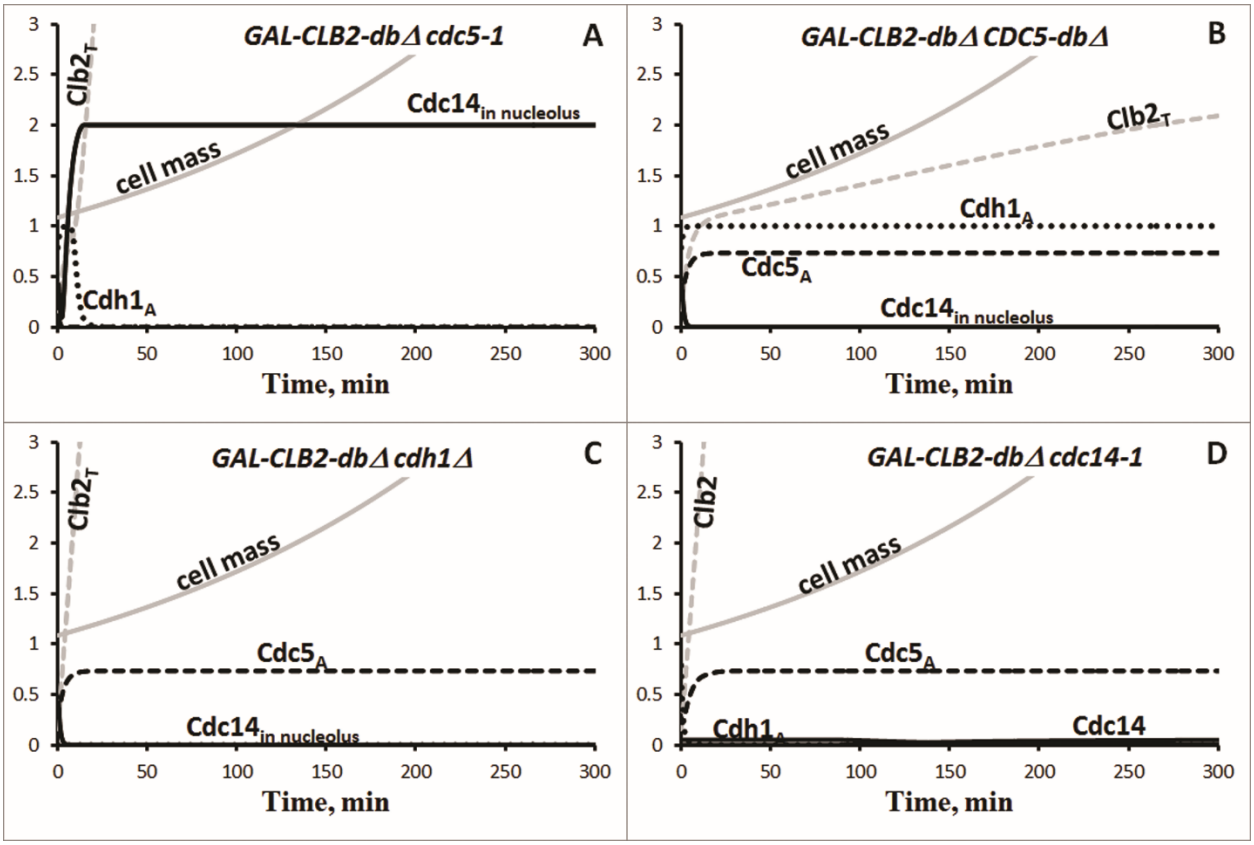

Figure S4. Cdc14 endocycles are blocked by mutations that disrupt the negative feedback loop Cdc5 → Cdc14 → Cdh1 ⊣ Cdc5.

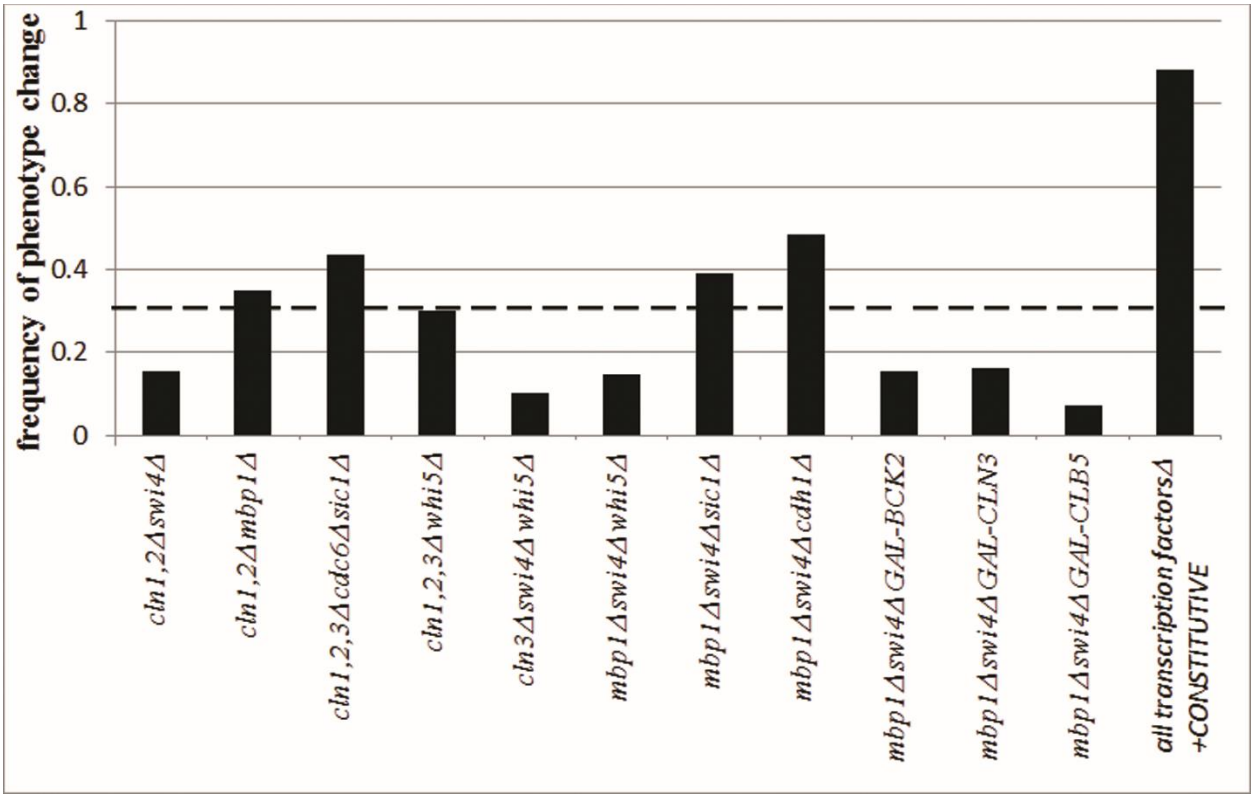

Figure S5. Robustness analysis for the predicted phenotypes of the strains in Table S9. Each bar on the histogram is assigned to a particular mutant strain and represents the probability that a parameter set consistent with the bench-mark strains predicts the phenotype opposite to the prediction in Table S9. Dashed line corresponds to the average frequency (f_{av} = 0.3).